NASA TECHNICAL NOTE

NASA TN D-4705

NASA TN D-4705

AN EXPERIMENTAL AND ANALYTICAL VIBRATION STUDY OF THIN CYLINDRICAL SHELLS WITH AND WITHOUT LONGITUDINAL STIFFENERS

by John L. Sewall and Eugene C. Naumann

Langley Research Center
Langley Station, Hampton, Va.

NATIONAL AERONAUTICS AND SPACE ADMINISTRATION • WASHINGTON, D. C. • SEPTEMBER 1968

AN EXPERIMENTAL AND ANALYTICAL VIBRATION STUDY OF THIN CYLINDRICAL SHELLS WITH AND WITHOUT LONGITUDINAL STIFFENERS

By John L. Sewall and Eugene C. Naumann

Langley Research Center
Langley Station, Hampton, Va.

NATIONAL AERONAUTICS AND SPACE ADMINISTRATION

For sale by the Clearinghouse for Federal Scientific and Technical Information
Springfield, Virginia 22151 – CFSTI price $3.00

AN EXPERIMENTAL AND ANALYTICAL VIBRATION STUDY OF THIN CYLINDRICAL SHELLS WITH AND WITHOUT LONGITUDINAL STIFFENERS

By John L. Sewall and Eugene C. Naumann
Langley Research Center

SUMMARY

Results of vibration tests are presented and compared with analytical results for aluminum-alloy cylindrical shells with and without external or internal integral longitudinal stiffeners for four end-support conditions. The stiffeners were of rectangular cross section and were closely spaced over the shell surface. Analytical results were obtained by application of the energy method employing the Rayleigh-Ritz procedure, in which longitudinal modal components were approximated by an arbitrary number of elementary beam-vibration functions chosen to satisfy prescribed end conditions.

Experimental and analytical results show the minimum frequencies of the externally stiffened shells, in all cases, to be significantly higher than the minimum frequencies of the corresponding internally stiffened shells. Agreement between measured and calculated frequencies was significantly improved when the analysis included local transverse bending stiffness due to the stiffeners, and additional beam modes for support conditions other than simply supported. The effect of including stiffener rotatory inertia in the analysis was found to be negligible in the present study.

Although this paper is primarily concerned with stringer-stiffened shells, applications of the analysis to two ring-stiffened shells are included to show the extent to which the averaged-stiffener assumption is valid for these configurations.

INTRODUCTION

In recent years, considerable interest has been shown in the elastic stability and vibrations of shells stiffened eccentrically (or unsymmetrically) by means of stringers and/or rings whose centroids lie inside or outside the shell surface. Test results reported in references 1 and 2 show increases by as much as a factor of 2 in axial buckling loads for cylindrical shells with externally mounted stringers, in contrast to such loads for internally mounted stringers.

Results such as these have stimulated a number of buckling and vibration studies of eccentrically stiffened shells. (See, for example, refs. 3 to 9.) In the analytical work reported in most of these studies, the middle surface of the shell wall is chosen as the reference surface, so that membrane and bending deformations of the stiffener with respect to this surface are coupled, thereby giving rise to the stiffener eccentricity effect. This is also the approach used by Flügge in reference 10 and by Baruch and Singer in references 11 and 12. As such, it differs from the equivalent-shell approach, in which the reference surface is the centroidal surface of the shell-stiffener combination, and eccentricity effects are explicitly ignored. (See, for example, refs. 13 to 16.)

The purpose of the present paper is to report comparisons of analytical and experimental frequencies and mode shapes of eccentrically stiffened and unstiffened cylindrical shells with various end-support conditions. The analysis of reference 5, which predicts the eccentricity effect for simply supported shells with closely spaced stiffeners, is extended to other end conditions. The Rayleigh-Ritz procedure is employed, with beam-vibration functions approximating the longitudinal modal components for simply supported, clamped, and free end conditions. Included also are approximations of the effects of transverse bending stiffness and rotatory inertia of the stiffeners. Three shells were vibration-tested under various end-support conditions. Two of these were integrally stiffened, with stringers lying either inside or outside the shell wall. The third model was unstiffened. Experimental results are compared with both the analytical results of the present paper and those of reference 5, as well as with the results of the equivalent-shell method of reference 13. Application of the present analysis is also made to the longitudinally stiffened shells of reference 15 and the ring-stiffened shells of references 14 and 16.

The experimental investigation is presented first and is followed by the analytical investigation and comparisons of experimental and analytical results. The paper is supplemented by two appendixes.

SYMBOLS

The units used for the physical quantities in this report are given both in the U.S. Customary Units and in the International System of Units (SI). Any consistent system of units may be used in the analysis.

A cross-sectional area of stiffener

A_{im}, B_{im}, E_{im}
F_{im}, G_{im}, H_{im}
$\alpha_{im}, \beta_{im}, \gamma_{im}$
ϵ_{im}, η_{im}
} elements of stiffness matrix in frequency equation

$b = h + r_F$ (see appendix A)

C_{12}, C_{66}
D_{12}, D_{66}
} stiffnesses for equivalent-shell method of analysis (see appendix B)

D shell bending stiffness, $\frac{E_c h^3}{12(1 - \mu^2)}$

D_x longitudinal bending stiffness in shell, including transverse effect of rings

D_y circumferential bending stiffness in shell, including transverse effect of stringers

D_1 transverse Poisson stiffness in bending (see eq. (2))

d center-to-center distance between stringers, measured along middle surface of shell (see fig. 6)

E Young's modulus

f circular frequency, $\frac{\omega}{2\pi}$, hertz

G shear modulus

h shell thickness

I moment of inertia of stiffener about its own centroid

I_C, I_{F1}, I_{F2}, I_S integrals defined in appendix A

I_o moment of inertia of stiffener about shell middle surface, $I + A\bar{z}^2$

$I_1, I_2, I_3, I_{41}, I_{42}$ integrals of longitudinal mode-shape functions (see definitions of determinant elements following eq. (9))

J	torsion constant of stiffener
J_e	polar moment of inertia of stiffener about shell middle surface
L	length of cylinder between end supports
l	center-to-center distance between rings (see fig. 6)
M,N,P,Q	integers
M_A	mass of shell-stiffener combination per unit area, $\rho_c h + \rho_s \frac{A_s}{d} + \rho_r \frac{A_r}{l}$
M_y	circumferential bending moment (see appendix A)
m	longitudinal mode number (see fig. 4)
N_i,N_m	beam eigenvalues (see table VI)
N_{xy}	in-plane shear stress resultant
n	circumferential mode number (see fig. 4)
R	radius to middle surface of shell (see fig. 6)
$\overline{R} = \frac{E_r A_r}{E_c h l}$	
r_F	fillet radius
r_S	one-half the stringer width
$\overline{S} = \frac{E_s A_s}{E_c h d}$	
T	kinetic energy (see eqs. (3) and (5))
t	time
U	strain energy in shell and stiffeners (see eq. (1))
u,v,w	longitudinal, circumferential, and radial (or normal) displacements, respectively (see fig. 6)

X_i, X_m longitudinal mode-shape functions

x,y,z longitudinal circumferential, and radial coordinates, respectively (fig. 6)

$\bar{z}$ distance of stiffener centroid from shell middle surface, positive for stiffener centroid outward

γ_i, γ_m eigenvalue properties of beam (see table VI)

$\overline{\Delta}$ frequency parameter, $\frac{R^2\omega^2\rho_c\left(1 - \mu^2\right)}{E_c}$

$\Lambda_r = 1 + \overline{R}\left(1 - \mu^2\right)$

$\Lambda_s = 1 + \overline{S}\left(1 - \mu^2\right)$

λ modal wavelength

μ Poisson's ratio for shell

ρ mass density

$\psi = \frac{h^2}{12R^2}$

ω angular frequency, $2\pi f$, radians/second

Subscripts:

c cylinder

i,m identifies longitudinal modal components

j,k denote jth ring and kth stringer, respectively (see eq. (3))

r ring

s stringer

T total (see eqs. (4))

Superscript:

T transpose of matrix

A comma followed by subscripts denotes partial differentiation with respect to the subscripts.

EXPERIMENTAL INVESTIGATION

Models

Three cylindrical models were used in this investigation, namely, (1) an unstiffened shell, (2) a shell with external longitudinal stiffeners, and (3) a shell with internal longitudinal stiffeners. These configurations were selected to evaluate (1) test procedures and boundary conditions (by using the unstiffened model) and (2) the effect of eccentrically located longitudinal stiffeners (by using the internally or externally stiffened model). The models were designed to have nominally the same radius to the middle surface of the isotropic shell, the same skin thickness and cylinder length, and, for the stiffened cylinders, the same stiffener cross section and spacing. The actual dimensions of the cylinders were determined by averaging as many as 60 discrete measurements over the whole cylinder. These values are given in table I.

Nominal dimensions and configurations of the models are shown in figure 1. The unstiffened model was fabricated in halves from nominal 0.025-inch-thick (0.635-mm) 6061-T6 aluminum-alloy sheet. The stiffened models were fabricated in halves by machining the integral shell-stiffener cross section from 3/8-inch-thick (9.525-mm) 6061-T6 aluminum-alloy plate. The halves were rolled to the proper curvature and welded to form the cylindrical shells, each having two longitudinal seams 180° apart. The stiffened cylinders contained 60 longitudinal stiffeners with their centers spaced 1.00 inch (25.4 mm) apart, as measured along the middle surface of the isotropic shell. For all the shells, the grain direction of the material was oriented along the longitudinal axis of the cylinder. After being welded, the cylinders were machined to the proper length with the ends parallel to each other and normal to the longitudinal axis.

Model Supports

Each model was tested under four sets of boundary conditions; they were (1) free-free, (2) simply supported, (3) clamped-free, and (4) clamped-clamped. A description of each set of boundary conditions follows.

Free-free conditions.- Free-free boundary conditions were simulated by suspending the model vertically with eight uniformly spaced soft suspensions. The suspensions used

were soft rubber bands fastened at one end with metal clips attached to fiber tabs cemented to the cylinder. The other end of each rubber band was fastened to an overhead panel with a length of string. Suspension-system—model frequencies were measured to be as follows: vertical – less than 2/3 hertz, horizontal – less then 1/2 hertz, and rotational – less than 1/2 hertz.

Simple-support conditions.- For simple-support tests, the model was oriented horizontally and supported internally and externally at each end by restraining rings having sharp tip radii as shown in the cross-sectional view of sketch a. Pressure-sensitive 0.006-inch-thick (0.1524-mm) teflon tape was affixed to each ring to reduce friction. This type of restraint permitted longitudinal motion of the model while it restrained deflections normal to the shell. It should be noted that motion normal to the shell between stiffeners was not restrained on the stiffened side of the shell. For the stiffened cylinders, small teflon-coated clips were inserted at three locations between adjacent stiffeners at each end to restrain any rotation of the model. Reference marks

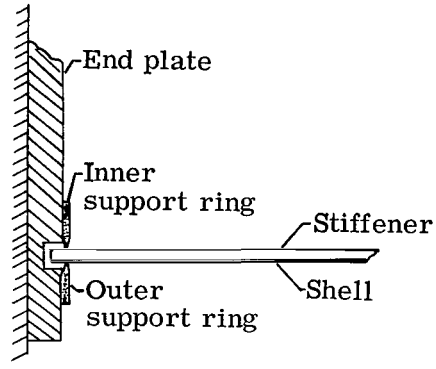

Sketch a.- Details of simple-support end condition.

on the unstiffened test model and adjacent fixtures were observed during testing to verify that the model was not rotating in the fixture. The ring fixtures also served a second purpose in that they caused the cylinder to retain a more nearly circular cross section throughout its length.

Clamped-free conditions.- The clamped-free end conditions were achieved by first alining one end of the cylinder in the annular groove in the end plate, using an inner support ring to keep the cylinder cross section circular, and then filling the annular groove with a low-melting-point, high-density potting material. Small spacers were set in the groove so that only 1/2 inch (12.7 mm) of the cylinder was immersed in the potting material. After the material solidified, the inner support ring was removed. The resulting clamped end condition is shown in sketch b.

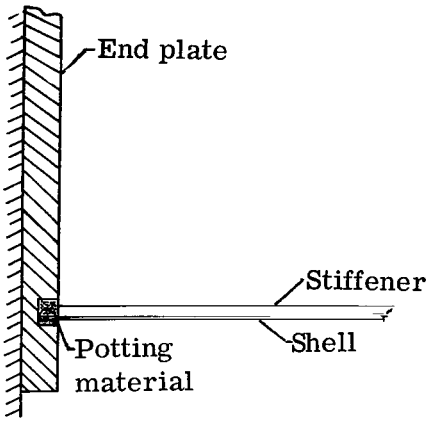

Sketch b.- Details of clamped end condition.

Clamped-clamped conditions.- The clamped-clamped end conditions were constructed by potting the free end of the clamped-free model after a similar technique of end alinement had been employed. Four 3/4-inch-diameter (19.05-mm) steel rods were used to set the end plates parallel and the proper distance apart. This whole rig was then alined to insure symmetry. The free end was held circular during potting by means of two sections of the outer support ring.

The strain gages used for modal identification (see instrumentation section) were also used to minimize misalinement in the two large plates anchoring the ends and to detect any load on the model induced by thermal expansions when the second end was potted. This was accomplished by balancing the strain-gage bridges prior to potting the the second end and by monitoring the gage readings throughout the mounting of the end plates. Although it was not possible to keep the models completely free of external loads, the magnitudes were thought to be minimal.

Model Excitation

A 1.5-pound-force (6.672-newton) electrodynamic shaker was used to induce vibrations in the cylinders. A variable-frequency sinusoidal oscillator signal was amplified and used to drive the shaker. The full 1.5-pound force of the shaker was never utilized, however. That is, the force applied to the cylinder was maintained at the lowest value that produced a clearly distinguishable signal on the monitoring instruments.

The shaker was suspended on a soft spring-string system so that only the mass of the shaker slug and the attachment device was added to the cylinder mass. Figure 2 is a photograph of a typical shaker installation. Identified in figure 2 are (1) soft spring-string suspension, (2) shaker, and (3) connecting rod and attachment device.

As shown in figure 2, two methods of shaker attachment were used. One employed a vacuum-cup fastener and the other, a mechanical fastener. The vacuum-cup attachment could be used for all tests, whereas the mechanical fastener could be used only when the stiffeners were exposed. For some test conditions, both attachment methods were used, and essentially no variation in results was obtained. Changing the attachment device and varying certain segments of the suspension system permitted the positioning of the shaker at essentially any point on the cylinder.

For tests conducted on the models with free ends, an air shaker, as described in reference 17, was used to excite the models for small values of m and n. An air shaker was necessary because of the appreciable stiffness and mass effects of the electrodynamic shaker on the model frequencies. (See, for example, refs. 18 and 19.)

Instrumentation

The detection and identification of vibratory modes in thin shells has been a problem for experimentalists for years. The additional mass of an accelerometer, velocity pickup, or other contact-type sensor very frequently influences nodal preference and, for mobile probes, can cause nodal rotation. Surface-strain measuring techniques have been affected in the past by very poor signal-to-noise ratios because of the low strain values associated with thin shells. Recent advances in electronic miniaturization and stabilization were incorporated in two methods of vibration detection and modal identification for this test program. One method measured surface strains with standard foil strain gages, and the other method used a noncontact, inductance-type proximity sensor.

The proximity-sensor system is described in detail in reference 20; however, for the reader's convenience, a brief description is included herewith. A schematic representation of this type of instrumentation, as used for the present investigation, is shown in figure 3. The inductance probe and its electronics produce a dc voltage which is proportional to the distance from the probe to the instantaneous position of the skin of the model. This voltage is processed to yield an average dc level (probe-displacement voltage) and an alternating voltage (proportional to deflection double amplitude). The average dc level is proportional to the mean distance between the probe and skin and is used in the servosystem. In this system, probe-displacement voltage is compared, both in magnitude and phase, with a predetermined reference voltage, and any difference is sent to a dc amplifier as an error signal. The amplified error signal is then used to drive the servomotor in the proper direction in order to keep the error signal at a minimum. The alternating amplitude voltage is processed by an ac-dc converter for presentation on an x-y plotter, or the signal can be fed directly into an oscilloscope.

In order to obtain a description of the cylinder vibration motions in a plane normal to the axis (or to the shell surface), the probe and servomotor were mounted on a

motorized trolley which ran on a circular track around the model so as to determine the circumferential mode shapes. Longitudinal mode shapes could be scanned by moving the track-trolley system along the axis of the cylinder. Circumferential and longitudinal mode shapes are defined by the indexes n and m, respectively, as shown in figure 4.

Longitudinal mode shapes were determined in a number of cases by both the strain gages and the proximity sensor in order to evaluate the agreement between these techniques. Because of the excellent agreement obtained, and in order to decrease the time required to obtain test data, the strain gages were used in lieu of moving the trolley-track system to determine the longitudinal mode shape for each frequency response. The differential dc amplifiers used in this system have very low noise levels and high gain; therefore, clear signals were obtained even for very low input force levels.

The general test procedure was as follows: (1) the oscillator frequency was slowly increased until a maximum signal was obtained from a motion-sensing transducer (either probe or strain-gage), (2) the longitudinal mode m was determined by switching through the series of strain gages, (3) the circumferential mode n was determined by requiring the proximity probe to traverse around the model, and (4) the model frequency was determined by an electronic counter which sampled the probe output.

Test Results

The experimental results obtained were resonant frequencies and associated longitudinal and circumferential modes as presented in tables II to V. In table III (free-free tests), it should be noted that for the two lowest longitudinal modes (m = 0 and 1) and small values of n, the frequencies obtained with the air shaker are generally lower than those obtained with the electrodynamic shaker. For completeness, both sets of data are included; however, it is thought that the frequencies obtained with the air shaker are more nearly correct over the range of n values covered.

Typical circumferential mode shapes, as obtained with the proximity-probe system, are shown in figure 5(a) for the internally stiffened cylinder with clamped-free end conditions. The dashed curve is a sine wave, and the somewhat irregular solid curve indicates the output displacements obtained from the proximity probe. The solid curve is discontinuous in the vicinity of the shaker because of clearance requirements. The difference between the theoretical and actual mode shapes is due, in part, to nonlinearities in the position-sensing potentiometer. Except for this difference, there is good agreement between the theoretical and actual mode shapes, which indicates that a single trigonometric function would be adequate to represent the circumferential mode shapes.

Typical longitudinal-mode-shape data obtained from the strain-gage system are shown in figure 5(b). The circular test point symbols represent strain-gage data, and the solid curves, results of calculations using elementary beam functions as taken from

reference 21. The data presented are for the internally stiffened shell with the clamped-clamped boundary conditions. The good agreement here between experimental and analytical mode shapes indicates that beam-vibration functions could be used to represent the longitudinal mode shapes.

For many m and n mode combinations, dual resonances (i.e., two frequencies with the same m and n values) were obtained, as indicated in tables II to V. An examination of the recorded n-mode shapes shows that the circumferential mode has two preferred orientations, one of which is rotated by $\lambda/4$ with respect to the other, λ being the modal wavelength. Whether these preferred orientations are due to construction defects or to rotational and translational energies of the stiffeners is not known. In either case, the phenomenon of dual resonances in nominally rotationally symmetric structures is well known, and the reader is referred to Tobias' work for further explanation. (See, for example, ref. 22.)

ANALYTICAL INVESTIGATION

Analytical shell frequencies and mode shapes presented in this paper were obtained by application of the well-known energy method employing the Rayleigh-Ritz procedure. Stringer and ring stiffeners are assumed to be spaced closely enough for their effects to be averaged (or "smeared") over the shell surface. Eccentricity effects due to stiffeners attached inside or outside the shell wall are explicitly taken into account. In-plane and radial shell displacements u, v, and w (fig. 6) are each assumed to be products of single-term circumferential modes and multiterm longitudinal (or axial) modes. The circumferential modes are trigonometric functions, and the longitudinal modes are beam-vibration functions, the choice of which enables consideration of various end conditions. The analysis is very similar to that of reference 5, but is somewhat broader in scope because of the consideration of end conditions other than simply supported and because of provision for the effects of transverse bending and rotatory inertia of the stiffeners.

Method of Analysis

Strain energy.- The coordinate system and notation used in the analysis are defined in figure 6. With the use of the linear strain-displacement relations of Novozhilov (ref. 23), the strain energy of a thin cylindrical shell reinforced by closely spaced rings and stringers may be written as follows:

$$U = \frac{E_c h}{2(1-\mu^2)} \int_0^{2\pi R} \int_0^L \left[u_{,x}^2 + \left(v_{,y} + \frac{w}{R}\right)^2 + 2\mu u_{,x}\left(v_{,y} + \frac{w}{R}\right) + \frac{1-\mu}{2}\left(u_{,y} + v_{,x}\right)^2 \right] dx\, dy$$

$$+ \frac{D}{2} \int_0^{2\pi R} \int_0^L \left[\frac{D_x}{D} w_{,xx}^2 + \frac{D_y}{D}\left(w_{,yy} - \frac{v_{,y}}{R}\right)^2 + \frac{2D_1}{D} w_{,xx}\left(w_{,yy} - \frac{v_{,y}}{R}\right) \right.$$

$$\left. + 2(1-\mu)\left(w_{,xy} - \frac{v_{,x}}{R}\right)^2 \right] dx\, dy + \frac{1}{2\ell} \int_0^{2\pi R} \int_0^L \left\{ E_r \left[A_r \left(v_{,y} + \frac{w}{R}\right)^2 \right. \right.$$

$$\left. \left. - 2\bar{z}_r A_r \left(v_{,y} + \frac{w}{R}\right)\left(w_{,yy} - \frac{v_{,y}}{R}\right) + I_{o_r}\left(w_{,yy} - \frac{v_{,y}}{R}\right)^2 \right] + G_r J_r \left(w_{,xy} - \frac{v_{,x}}{R}\right)^2 \right\} dx\, dy$$

$$+ \frac{1}{2d} \int_0^{2\pi R} \int_0^L \left[E_s \left(A_s u_{,x}^2 - 2\bar{z}_s A_s u_{,x} w_{,xx} + I_{o_s} w_{,xx}^2 \right) + G_s J_s \left(w_{,xy} - \frac{v_{,x}}{R}\right)^2 \right] dx\, dy \tag{1}$$

The first integral gives the shell extensional energy and the second integral gives the shell bending energy, $\frac{E_c h}{1-\mu^2}$ being the extensional stiffness and $D = \frac{E_c h^3}{12(1-\mu^2)}$ being the bending stiffness. The last two integrals contain both extensional and bending energies for closely spaced rings and stringers, and the eccentricity effects are explicitly accounted for through the coupling of these two energies in the terms involving the distances $\bar{z}_r$ and $\bar{z}_s$. A comma followed by subscripts denotes partial differentiation with respect to the subscripts.

Equation (1) reduces to the strain-energy expressions in reference 5 when $\frac{D_x}{D} = \frac{D_y}{D} = 1$, when $\frac{D_1}{D} = \mu$, and when the Donnell-type approximations are used for two of the strain-displacement relations $\left(\text{i.e., when } w_{,yy} - \frac{v_{,y}}{R} \approx w_{,yy} \text{ and } w_{,xy} - \frac{v_{,x}}{R} \approx w_{,xy}\right)$.

Transverse bending effects.- The term D_x in equation (1) is the longitudinal bending stiffness in the shell including the transverse stiffness contributed by the finite width of the rings, and D_y is the shell circumferential bending stiffness including the transverse stiffness contributed by the finite width of the stringers. The term D_1 is a so-called transverse Poisson stiffness in the shell and is approximated by the relation

$$\frac{D_1}{D} \approx \frac{\mu}{2}\left(\frac{D_x}{D} + \frac{D_y}{D}\right) \tag{2}$$

for a stringer-and-ring-reinforced shell of isotropic material. Consideration of the effects of these ratios in the present study is based on the work of reference 24. Details on estimations of the ratio magnitudes are given in appendix A. It is shown that in a shell stiffened by stringers or rings, $\frac{D_x}{D}$ or $\frac{D_y}{D} \geqq 1$. Thus, from equation (2), $\frac{D_1}{D} \geqq \mu$.

The effects of stringers and/or rings on the shell torsional stiffness (fourth term of second integral in eq. (1)) are neglected.

Kinetic energy.- The kinetic energy of a stringer-and-ring-stiffened cylindrical shell, with rotatory inertia of the stiffeners included, may be written in the following general form for M rings and N stringers:

$$T = \frac{\rho_c h}{2}\int_0^{2\pi R}\int_0^{L}\left(u_{,t}^2 + v_{,t}^2 + w_{,t}^2\right)dx\,dy$$

$$+\sum_1^M\left\{\frac{\rho_r}{2}\int_0^{2\pi R}\int_{A_r}\left[u_{T,t}^2 + v_{T,t}^2 + (x - x_r)^2 w_{,tx}^2 + w_{T,t}^2\right]dA_r\,dy\right\}_j$$

$$+\sum_1^M\left\{\frac{\rho_s}{2}\int_0^{L}\int_{A_r}\left[u_{T,t}^2 + v_{T,t}^2 + (y - y_s)^2\left(\frac{1}{R}v_{,t} - w_{,ty}\right)^2 + w_{T,t}^2\right]dA_s\,dx\right\}_k \qquad (3)$$

The total linear velocities in equation (3) are given by

$$\left.\begin{aligned} u_{T,t} &= u_{,t} - zw_{,tx} \\ v_{T,t} &= v_{,t} + z\left(\frac{1}{R}v_{,t} - w_{,ty}\right) \\ w_{T,t} &= w_{,t} \end{aligned}\right\} \qquad (4)$$

The third terms in both of the summations in equation (3) are rotational terms that are considered small in comparison with the total velocities. No separate evaluation of these terms (apart from the total-rotatory-inertia evaluation) was made in this study.

Substitution of equations (4) into equation (3) and integration over the stiffener cross-sectional areas leads to the following form of the kinetic energy of a cylindrical shell with closely spaced stiffeners:

$$T = \frac{\rho_c h}{2}\int_0^{2\pi R}\int_0^{L}\left(u_{,t}^2 + v_{,t}^2 + w_{,t}^2\right)dx\,dy + \frac{\rho_r}{2l}\int_0^{2\pi R}\int_0^{L}\left\{A_r\left(u_{,t}^2 + v_{,t}^2 + w_{,t}^2\right)\right.$$

$$\left. + 2A_r\bar{z}_r\left[-u_{,t}w_{,tx} + v_{,t}\left(\frac{1}{R}v_{,t} - w_{,ty}\right)\right] + J_{e_r}w_{,tx}^2 + I_{o_r}\left(\frac{1}{R}v_{,t} - w_{,ty}\right)^2\right\}dx\,dy$$

$$+ \frac{\rho_s}{2d}\int_0^{2\pi R}\int_0^{L}\left\{A_s\left(u_{,t}^2 + v_{,t}^2 + w_{,t}^2\right) + 2A_s\bar{z}_s\left[-u_{,t}w_{,tx} + v_{,t}\left(\frac{1}{R}v_{,t} - w_{,ty}\right)\right]\right.$$

$$\left. + I_{o_s}w_{,tx}^2 + J_{e_s}\left(\frac{1}{R}v_{,t} - w_{,ty}\right)^2\right\}dx\,dy \qquad (5)$$

where J_{e_r} and J_{e_s} are polar moments of inertia of the ring and stringer cross-sectional areas about the shell middle surface.

Equation (5) reduces to equation (9) of reference 5 when the in-plane shell velocities $u_{,t}$ and $v_{,t}$ and the total velocities $u_{T,t}$ and $v_{T,t}$ are zero and when simple harmonic motion is assumed in equation (5).

Modal functions.- The expressions assumed for the in-plane and radial displacements u, v, and w are

$$\left.\begin{aligned} u(x,y,t) &= \cos\frac{ny}{R}\sum_{m=P}^{Q} u_m(t)X'_m(x) \\ v(x,y,t) &= \sin\frac{ny}{R}\sum_{m=P}^{Q} v_m(t)X_m(x) \\ w(x,y,t) &= \cos\frac{ny}{R}\sum_{m=P}^{Q} w_m(t)X_m(x) \end{aligned}\right\} \qquad (6)$$

where $P = 0$ for the free-free end condition and $P = 1$ for other end conditions, Q is the number of longitudinal modes, and $X'_m = \frac{dX_m}{dx}$. The modal function X_m is a beam-vibration function chosen to satisfy a prescribed set of end conditions, and u_m, v_m, and w_m are generalized coordinates or amplitude functions. The choice of a beam function for X_m allows some simplification in the analysis through the orthogonality properties

$$\int_0^L X_i X_m \, dx = \int_0^L X_i'' X_m'' \, dx = 0 \qquad (i \neq m) \qquad (7)$$

The end conditions of simply supported cylindrical shells are fully satisfied with $X_m = \sin \frac{m\pi x}{L}$ and each of equations (6) reduced to a single term.

For other end conditions considered in this paper, equations (6) provide convenient general forms which are satisfactory within certain limitations inherent in the Rayleigh-Ritz procedure. Specifically, equations (6) do not allow all possible rigid-body motions. Moreover, when the end of the shell is clamped, there is the contradiction of having both $v = 0$ and $N_{xy} = \frac{E_c h}{2(1 + \mu)}\left(u_{,y} + v_{,x}\right) = 0$ at the end, when X_m is approximated by a beam function. The full effects of these limitations, particularly the last one, have not been evaluated in this study.

Equations of essentially the same forms as equations (6), with X_m represented by beam functions, have been used in reference 25 for clamped-clamped cylindrical shells (for $m \geqq 1$) and in reference 26 for free-free cylindrical shells (for $m \geqq 2$).

General form of frequency equation.- With the substitution of equations (6) into equations (1) and (5) and the assumption of simple harmonic motion of frequency ω, the equations of motion are obtained from the three sets of relations

$$\frac{\partial}{\partial \bar{u}_i}\left[U(x,y) - \omega^2 T(x,y)\right] = \frac{\partial}{\partial \bar{v}_i}\left[U(x,y) - \omega^2 T(x,y)\right] = \frac{\partial}{\partial \bar{w}_i}\left[U(x,y) - \omega^2 T(x,y)\right] = 0 \qquad (8)$$

on the basis of $u_i(t) = \bar{u}_i e^{i\omega t}$, $v_i(t) = \bar{v}_i e^{i\omega t}$, and $w_i(t) = \bar{w}_i e^{i\omega t}$ where the exponent $i = \sqrt{-1}$. The operations represented by these equations lead to the familiar eigenvalue-eigenvector formulation which may be expressed in the following matrix form:

Stiffness matrix Mass matrix

$$\left[\begin{bmatrix} A_{im} & B_{im} & E_{im} \\ B_{im}^T & F_{im} & G_{im} \\ E_{im}^T & G_{im}^T & H_{im} \end{bmatrix} - \bar{\Delta}\begin{bmatrix} \alpha_{im} & 0 & \epsilon_{im} \\ 0 & \beta_{im} & \eta_{im} \\ \epsilon_{im}^T & \eta_{im}^T & \gamma_{im} \end{bmatrix}\right]\begin{Bmatrix} \bar{u} \\ \bar{v} \\ \bar{w} \end{Bmatrix} = \begin{Bmatrix} 0 \\ 0 \\ 0 \end{Bmatrix} \qquad (9)$$

where $\bar{\Delta} = \frac{R^2\omega^2\rho_c\left(1 - \mu^2\right)}{E_c}$, and each element of the matrices represents a submatrix whose elements are specified as follows:

$$A_{im} = R^2 \Lambda_s I_3 + n^2 I_2 \frac{1 - \mu}{2}$$

$$B_{im} = nR\left(\mu I_{41} - \frac{1 - \mu}{2} I_2\right)$$

$$E_{im} = R\left[\mu I_{41} - R\bar{z}_s \bar{S} I_3 (1 - \mu^2)\right]$$

$$F_{im} = n^2 \Lambda_r I_1 + R^2 \frac{1 - \mu}{2} I_2 + (1 - \mu^2)\left\{\frac{\psi}{1 - \mu^2}\left[n^2 \frac{D_y}{D} I_1 + 2(1 - \mu) R^2 I_2\right]\right.$$

$$\left. + n^2 I_1\left(2 \frac{\bar{z}_r}{R} \bar{R} + \frac{E_r I_{o_r}}{E_c h \ell R^2}\right) + \frac{I_2}{E_c h}\left(\frac{G_s J_s}{d} + \frac{G_r J_r}{\ell}\right)\right\}$$

$$G_{im} = nI_1\left[\Lambda_r + \bar{R} n^2 \frac{\bar{z}_r}{R}(1 - \mu^2)\right] + n(1 - \mu^2)\left\{\frac{\psi}{1 - \mu^2}\left[n^2 \frac{D_y}{D} I_1 - R^2 \frac{D_1}{D} I_{42} + 2(1 - \mu) R^2 I_2\right]\right.$$

$$\left. + I_1\left(\frac{\bar{z}_r}{R} \bar{R} + n^2 \frac{E_r I_{o_r}}{E_c h \ell R^2}\right) + \frac{I_2}{E_c h}\left(\frac{G_s J_s}{d} + \frac{G_r J_r}{\ell}\right)\right\}$$

$$H_{im} = I_1 + R^4 \psi\left[\frac{D_x}{D} I_3 + \frac{D_y}{D}\left(\frac{n}{R}\right)^4 I_1 - \frac{D_1}{D}\left(\frac{n}{R}\right)^2 (I_{41} + I_{42}) + 2(1 - \mu)\left(\frac{n}{R}\right)^2 I_2\right]$$

$$+ \frac{(1 - \mu^2) R^2}{E_c h}\left[\frac{E_s I_{o_s}}{d} I_3 + \left(\frac{n}{R}\right)^4 \frac{E_r I_{o_r}}{\ell} I_1\right] + (1 - \mu^2) \bar{R} I_1\left(1 + 2n^2 \frac{\bar{z}_r}{R}\right)$$

$$+ n^2 (1 - \mu^2) \frac{I_2}{E_c h}\left(\frac{G_s J_s}{d} + \frac{G_r J_r}{\ell}\right)$$

$$\alpha_{im} = I_2\left(1 + \frac{\rho_s A_s}{\rho_c h d} + \frac{\rho_r A_r}{\rho_c h \ell}\right)$$

$$\epsilon_{im} = \frac{-I_2}{\rho_c h}\left(\frac{\rho_s \bar{z}_s A_s}{d} + \frac{\rho_r \bar{z}_r A_r}{\ell}\right)$$

$$\beta_{im} = I_1\left[1 + \frac{\rho_s}{\rho_c hd}\left(A_s + 2A_s\frac{\bar{z}_s}{R} + \frac{Je_s}{R^2}\right) + \frac{\rho_r}{\rho_c h\ell}\left(A_r + 2A_r\frac{\bar{z}_r}{R} + \frac{Io_r}{R^2}\right)\right]$$

$$\eta_{im} = \frac{nI_1}{\rho_c hR}\left[\frac{\rho_s}{d}\left(A_s\bar{z}_s + \frac{Je_s}{R}\right) + \frac{\rho_r}{\ell}\left(A_r\bar{z}_r + \frac{Io_r}{R}\right)\right]$$

$$\gamma_{im} = \frac{M_A}{\rho_c h}I_1 + \frac{\rho_s}{\rho_c hd}\left[\left(\frac{n}{R}\right)^2 Je_s I_1 + Io_s I_2\right] + \frac{\rho_r}{\rho_c h\ell}\left[Je_r I_2 + \left(\frac{n}{R}\right)^2 Io_r I_1\right]$$

The quantities I_1, I_2, I_3, I_{41}, and I_{42} are integrals of various products of X_m and its derivatives. Evaluations of these integrals are given in table VI(a) for the end conditions considered in the present investigation and were taken from reference 27.

The frequency equation is obtained from equation (9) by requiring that the determinant of the coefficients of the amplitude functions $\bar{u}_i$, $\bar{v}_i$, and $\bar{w}_i$ vanish. Once the frequencies are obtained, amplitude ratios (or eigenvectors) and, in turn, the longitudinal mode shapes, may be found in a straightforward manner. The circumferential mode shapes are, of course, sinusoidal in accordance with equations (6).

Analytical Results

The analysis just described was applied to the unstiffened and stringer-stiffened cylindrical shells which were vibration tested in this investigation, and results showing particular effects are presented in figure 7. Other results, including those for the models of references 14 and 16, are considered subsequently in comparisons with experimental results.

Transverse bending effects.- Analytical results showing the effects of increased circumferential shell bending stiffness are shown in figure 7(a). Because of the stringers, this stiffness was increased by 19.7 percent $\left(\text{i.e., } \frac{D_y}{D} = 1.197\right)$ on the basis of the method of reference 24 as applied in appendix A. Since there were no rings on these shells, there was no increase in longitudinal shell bending stiffness; thus, $\frac{D_x}{D} = 1.00$. Therefore, from equation (2), with $\mu = 0.315$, the cross-coupling stiffness ratio D_1/D was 0.346. As was expected, the increase of D_y/D above 1.00 had a larger effect at larger values of n, where, as shown by Arnold and Warburton in reference 28, the bending contribution to the frequency predominates over the extensional contribution. Figure 7(a) shows that at $n = 15$, the frequency increased by about 9 percent for $m = 1$, 5.8 percent for $m = 2$, and 3.3 percent for $m = 3$. Figure 7(a) also shows that the frequencies

calculated by the present analysis for $\frac{D_y}{D} = 1.00$ are essentially the same as those calculated by the method of reference 5 except at low values of n, where the differences are largely due to neglect of in-plane velocities $u_{,t}$ and $v_{,t}$ in reference 5.

Effects of stiffener rotatory inertia.- Figure 7(b) shows the effects of stiffener rotatory inertia. These effects can be seen by comparing frequencies based on equation (9) with those obtained with only mass-inertia terms retained in the mass matrix (i.e., with all terms involving eccentricity and moments of inertia omitted from the mass matrix). As indicated in the figure, the stiffener rotatory inertia had a negligible effect on frequency over most of the range of m and n values. The largest frequency drop was less than 1.5 percent for the externally stiffened shell (m = 3, n = 15) and less than 2.7 percent for the internally stiffened shell (not shown).

Effects of modal coupling.- Since figures 7(a) and 7(b) apply to the simply supported end conditions, only a single modal product is required for each of the displacements in equations (6), as has been previously noted. Consequently, each submatrix in equation (9) reduces to a single element since, with $X_m = \sin \frac{m\pi x}{L}$, the integrals I_1, I_2, I_3, I_{41}, and I_{42} vanish when $i \neq m$, as is shown in table VI(a).

For end conditions other than simply supported, more than one modal product in each of equations (6) was generally required to obtain converged solutions, as is shown in figure 7(c). Solutions were considered converged when the frequencies were negligibly changed by the introduction of an additional modal product in each of the displacements u, v, and w. On this basis, the calculated frequencies of the clamped-free models converged satisfactorily with 7 modal products for m = 1 to 3; the clamped-clamped models, with 8 modal products for m = 1 to 3 (m = 3 not shown in fig. 7(c)); and the free-free models, with 9 modal products for m = 2 and 3. For the two lowest free-free mode numbers (m = 0 and 1), only a single modal product in each displacement was needed for convergence over most of the range of n values with the exception of n = 10 to 15 for m = 1. The close agreement in figure 7(c) between the solid and dashed curves at minimum frequencies indicates that single beam-mode displacement representations can give adequate approximations to these frequencies for shells with clamped and/or free ends, within the limitations of the analysis noted earlier.

COMPARISON OF EXPERIMENTAL AND ANALYTICAL RESULTS

Calculated converged frequencies are compared with measured frequencies in figures 8 to 11 for both the unstiffened and longitudinally stiffened models of the present test program. Comparisons of results of the present analysis with other test results are shown in figures 12 and 13. These results are discussed in the following sections.

Unstiffened Shell

Calculated and measured frequencies for the unstiffened shell with various end conditions are compared in the (a) parts of figures 8 to 11. Good agreement between theory and experiment is evident in figures 8(a), 9(a), and 11(a) for the simply supported, free-free, and clamped-free end conditions, respectively, over the entire test ranges of m and n values. In figure 9(a), the measured frequencies for the two lower free-free modes, $m = 0$ and 1, are those obtained with the air shaker. All other measured frequencies in figures 8 to 11 were obtained with the electrodynamic shaker.

For the clamped-clamped shell (fig. 10(a)), the agreement between measured and calculated frequencies is generally satisfactory over a wide range of m and n values, but is clearly not as good as the agreement for the other three end conditions. This is particularly true at low n values where the calculated frequencies are almost 10 percent higher than the experimental frequencies (at $m = 1$, $n = 5$ and at $m = 2$, $n = 7$). These differences are thought to be mainly due to the in-plane shear contradiction inherent in the analysis and, to a lesser extent, to some external loading (due to the potting of the ends) which could not be completely eliminated from the model. The in-plane shear contradiction can be removed by assuming that the longitudinal components of the in-plane displacements u and v can be expressed by functions which are more general than those in equations (6) and which are not beam functions. These alternate assumptions and an evaluation of them are beyond the scope of the present paper.

The comparisons in the (a) parts of figures 8 to 11 indicate that the displacement assumptions of equations (6), together with the beam-vibration functions representing the longitudinal components, give satisfactory frequencies of an unstiffened cylindrical shell for a wide range of end-support conditions.

Eccentrically Stiffened Shells

Present tests.- The (b) parts of figures 8 to 11 show the frequencies of the externally stiffened shells to be generally higher than those of the internally stiffened shells for all the end conditions considered. The minimum frequencies of the externally stiffened shells were higher than those of the internally stiffened shells by about 34 percent for the simply supported model, 35 percent for the free-free model (for $m = 2$), 39 percent for the clamped-clamped model, and 21 percent for the clamped-free model. Larger increases are evident for higher order longitudinal modes. The good agreement between measured and calculated frequencies for the simply supported shells as well as for the shells having other end conditions confirms the existence of the eccentricity effect as predicted analytically in reference 5.

The (b) parts of figures 8 to 11 also show that elementary beam-vibration functions are satisfactory approximations to the longitudinal components of the mode shapes of the

cylindrical shell-stringer combinations for end-support conditions involving clamped and free ends.

As in the case of the unstiffened shell, the agreement between measured and calculated frequencies of the stiffened shells is better for the simply supported, free-free, and clamped-free models (figs. 8(b), 9(b), and 11(b), respectively) than for the clamped-clamped models (fig. 10(b)). The closer agreement for the internally stiffened shell than for the externally stiffened shell in figure 10(b) is not readily explainable, although the externally stiffened shell may have been subjected to more external loading than the internally stiffened shell.

Further confirmation of the eccentricity effect is provided in figure 8(b) by a comparison of the experimental and analytical frequencies of the present paper with the frequencies obtained by the equivalent-shell analysis of reference 13 and appendix B. This theory does not explicitly account for stiffener eccentricity, as does the present analysis, and, as a result, gives frequencies roughly midway between those of the externally and internally stiffened shells at low values of n. This trend is typical of trends found for other end conditions and is the same type of result as that found by Baruch and Singer in studies of the buckling of ring-stiffened cylindrical shells under hydrostatic pressure. (See ref. 11, for example.)

Other tests.- Figure 12 shows a comparison of two sets of calculated frequencies with measured frequencies for one of the stringer-stiffened, simply supported models of reference 15. These models were made of 0.0183-inch-thick (0.464-mm) sheet steel and had four and eight internal stringers of hat-shaped cross section. The values shown in figure 12 are for the eight-stringer model. The experimental frequencies, represented by the test point symbols, agree closely, at least for low values of m, with the calculated frequencies of the present analysis, represented by the solid curves. The dashed curves represent frequencies calculated by the equivalent-shell analysis of reference 13. A comparison of these equivalent-shell results with the results of the present analysis and the experimental data of reference 15 shows that the effects of stiffener eccentricity in this case are considerably smaller than the effects found in figure 8(b) for the integrally stiffened models of the present tests.

Applications of Analysis to Ring-Stiffened Shells

Although this paper is primarily concerned with stringer-stiffened shells, calculated frequencies showing the extent to which the analysis is applicable to ring-stiffened shells are also included. These calculated frequencies were obtained for the ring-stiffened shells vibration-tested in references 14 and 16 and are compared with measured frequencies in figure 13. The comparisons shown in figures 13(a) and 13(b) apply to shells with 19 and 11 small integral ring stiffeners, the data having been taken from

references 16 and 14, respectively. Clearly, the agreement between theory and experiment is satisfactory for values of n up to and including the n value for minimum frequency, but deteriorates considerably as n increases further. This indicates that the assumption that the stiffener properties can be averaged or "smeared" over the shell surface is satisfactory for a cylindrical shell with closely spaced rings for a limited range of n values bracketing the minimum-frequency condition. For the clamped-clamped shell of figure 13(b), convergence to the analytical frequencies was established for the same number of modal products used for the stringer-stiffened clamped-clamped shell in figure 7(c). Actually, only a single modal product was needed for convergence at $n \geqq 6$ in figure 13(b). It may also be of interest to note that the analytical frequencies in figure 13(b) are in very close agreement with those calculated in reference 14 on the basis of an equivalent-shell approach.

CONCLUSIONS

Results of vibration tests are presented and compared with analytical results for cylindrical shells with and without external or internal longitudinal stiffeners for four sets of end-support conditions. The shells were made of aluminum alloy and were integrally stiffened by closely spaced stringers of rectangular cross section. The analytical results were obtained by application of the energy method employing the Rayleigh-Ritz procedure. The stringers were averaged or "smeared" over the surface of the shell. The circumferential modal components used were single-term trigonometric functions, and the longitudinal components were approximated by an arbitrary number of elementary beam-vibration functions chosen to satisfy prescribed end conditions. Analytical results are also included for two ring-stiffened shells for which experimental data are available.

From the results of this study, the following conclusions appear to be valid:

1. The effect of stiffener eccentricity, or one-sidedness with respect to the shell middle surface, as predicted in the vibration analysis of NASA TN D-3010 for a simply supported cylindrical shell, is confirmed not only for simply supported end conditions, but also for other end conditions. Specifically, the minimum frequencies of the shell with external stringers were higher than those of the shells with internal stringers by about 34 percent for the simply supported model, 35 percent for the free-free model (for the family of modes with two circumferential nodes, i.e., $m = 2$), 39 percent for the clamped-clamped model, and 21 percent for the clamped-free model.

2. Elementary beam-vibration functions are satisfactory approximations to the longitudinal components of the mode shapes of the cylindrical shell-stiffener combination for end-support conditions involving clamped and free ends. Improved agreement between measured and calculated frequencies and mode shapes may be obtained for end

conditions other than simply supported by increasing the number of modal products in the analysis, in accordance with the Rayleigh-Ritz procedure, until converged solutions are obtained. The possibility of obtaining adequate approximations to the minimum frequencies on the basis of single beam-mode representations of the displacements is indicated for shells with clamped and/or free ends.

3. Good agreement between theory and experiment also depends on including local transverse bending stiffness due to the stiffeners, and this stiffness is, in general, not negligible but becomes significant for higher-order circumferential modes.

4. On the basis of the present study, stiffener rotatory inertia appears to have a negligible effect.

5. The assumption that the stiffener properties can be averaged (or "smeared") over the shell surface is satisfactory for a cylindrical shell with closely spaced rings for a small range of circumferential wave lengths (n) bracketing the minimum frequency condition.

Langley Research Center,
National Aeronautics and Space Administration,
Langley Station, Hampton, Va., March 20, 1968,
124-08-05-08-23.

APPENDIX A

ESTIMATION OF LOCAL TRANSVERSE BENDING STIFFNESS IN A CYLINDRICAL SHELL WITH CLOSELY SPACED STIFFENERS

This appendix contains pertinent details on the estimated increase in shell bending stiffness due to the presence of the stiffeners in a ring- and/or stringer-stiffened cylindrical shell. This estimation is based on the work of Huffington, Schumacher, and Irwin in reference 24 and is specifically concerned with the stringer-stiffened shells of the present investigation.

By making use of equation (37) of reference 24, the increase in circumferential bending stiffness in the shell due to the stringers may be expressed by the relation

$$\frac{D_y}{D} = \frac{1}{\frac{h^3}{d}\int_{-d/2}^{d/2} \frac{dy}{\left[h(y)\right]^3}} \tag{A1}$$

The derivation of this expression is based on the requirement that the strain energy in a typical region of the actual stiffened section be equal to the strain energy in the corresponding region of a hypothetical orthotropic section when both of these regions are subjected to the same loading and boundary conditions. This so-called strain-energy criterion involves the selection of a variable thickness $h(y)$ through the shell-stiffener section that is assumed to be equivalent to the actual stiffened section in its resistance to the loading imposed upon it. Equation (A1) is limited to the case of pure bending, and the stresses are assumed to vary linearly through the effective thickness, with the neutral surface occurring at the midheight of the stiffener-shell combination. The choice of $h(y)$ is somewhat arbitrary, and recommendations are given in reference 24 for some typical configurations. However, none of these recommendations give a clear indication of how to approximate the effective thickness through an integral stiffener having generous fillets such as those in the present study. A "generous" fillet is one in which the maximum strain occurs at the free surface.

A distribution of $h(y)$ that was considered reasonable for these models is one involving a succession of quarter-circular arcs through the stiffener and fillets. This distribution is illustrated in the following sketch (sketch c), where the shaded region is considered as ineffective in determining $h(y)$:

APPENDIX A

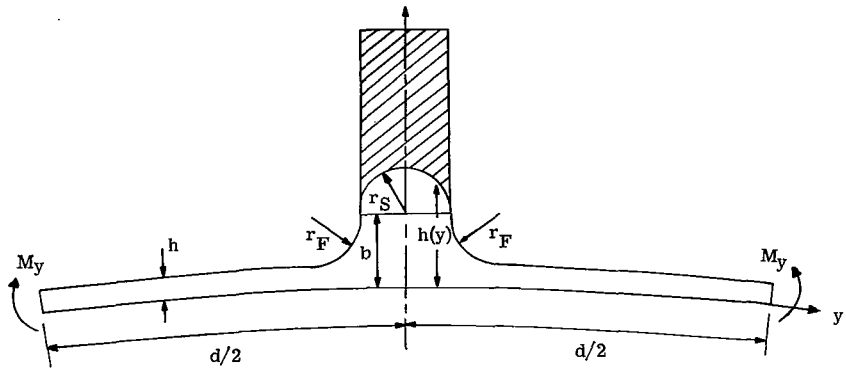

Sketch c.- Details of stringer-shell juncture.

The symbol M_y represents the circumferential bending moment assumed to be acting on this section.

With h(y) chosen as shown in sketch c, the integral in equation (A1) may be considered as the sum of four separate integrals, as follows:

$$\int_{-d/2}^{d/2} \frac{dy}{[h(y)]^3} = I_C + I_{F1} + I_S + I_{F2} \tag{A2}$$

where

$$I_C = \frac{1}{h^3}\left[\int_{-d/2}^{-(r_F+r_S)} dy + \int_{r_F+r_S}^{d/2} dy\right]$$

$$I_{F1} = \int_{-(r_F+r_S)}^{-r_S} \frac{dy}{\left[b - \sqrt{r_F^2 - (y + r_F + r_S)^2}\right]^3}$$

$$I_S = \int_{-r_S}^{r_S} \frac{dy}{\left[b + \sqrt{r_S^2 - y^2}\right]^3}$$

$$I_{F2} = \int_{r_S}^{r_F+r_S} \frac{dy}{\left[b - \sqrt{r_F^2 - (y - r_F - r_S)^2}\right]^3}$$

with

$$b = h + r_F$$

The first of these integrals represents the contribution of the shell between the stringers and is given by

$$I_C = \frac{d - 2(r_F + r_S)}{h^3} \tag{A3}$$

Clearly, for the isotropic shell with no stringers, the value of this integral becomes d/h^3, and the value of D_y/D is unity. The other three integrals in equation (A2) represent the contributions of the fillets and the stringer to the transverse increase in shell bending stiffness, $\frac{D_y}{D} > 1$. The integrals I_{F1} and I_{F2} apply to fillets to the left and right, respectively, of the stiffener in sketch c. The integral I_S represents the contribution of the stiffener itself. These three integrals may be evaluated to obtain the following closed forms by employing simple trigonometric substitutions and by differentiating under the integral sign:

$$I_{F1} = I_{F2} = I_F = \frac{r_F}{2}\left[\frac{b^2 + r_F^2}{b\left(b^2 - r_F^2\right)^2} + \frac{b}{\left(b - r_F\right)^2\left(b + r_F\right)^2} + \frac{6br_F}{\left(b^2 - r_F^2\right)^{5/2}} \tan^{-1}\sqrt{\frac{b + r_F}{b - r_F}}\right] \tag{A4}$$

$$I_S = r_S\left[\frac{b^2 + r_S^2}{b\left(b^2 - r_S^2\right)^2} + \frac{b}{\left(b - r_S\right)^2\left(b + r_S\right)^2} - \frac{6br_S}{\left(b^2 - r_S^2\right)^{5/2}} \tan^{-1}\sqrt{\frac{b - r_S}{b + r_S}}\right] \tag{A5}$$

Thus, in terms of equations (A3), (A4), and (A5), equation (A1) may be written as

$$\frac{D_y}{D} = \frac{1}{\frac{h^3}{d}\left(I_C + 2I_F + I_S\right)} \tag{A6}$$

By making use of the values of h, r_F, r_S, and d, as given in table I, the following values of D_y/D are obtained:

$$\frac{D_y}{D} = 1.197 \text{ for the externally stiffened shell}$$

$$\frac{D_y}{D} = 1.195 \text{ for the internally stiffened shell}$$

The analytical frequencies given in figures 8 to 11 are based on these values.

With the semicircular variation of h(y) through the stiffener reduced to a constant height $b = r_F + h$, as shown in sketch c, the integral I_S becomes simply

$$I_S = \int_{-r_S}^{r_S} \frac{dy}{b^3} = \frac{2r_S}{b^3}$$

and D_y/D is reduced accordingly. For example, the foregoing ratios when based on this approximation become

$\frac{D_y}{D} = 1.195$ for the externally stiffened shell

$\frac{D_y}{D} = 1.192$ for the internally stiffened shell

For a given shell-stringer geometry, the maximum stiffness increase may be obtained by allowing the thickness $h(y)$ to become infinite for both fillets and stringer. In this case, $I_F = I_S = 0$, and equation (A6) reduces to

$$\frac{D_y}{D} = \frac{1}{1 - \frac{2(r_F + r_S)}{d}} \tag{A7}$$

which gives $\frac{D_y}{D} = 1.29$ when based on the data in table I.

For a stringer without fillets, and with $h(y)$ equal to a constant b through the stringer width,

$$\frac{D_y}{D} = \frac{1}{1 - \frac{2r_S}{d}\left(1 - \frac{h^3}{b^3}\right)} \tag{A8}$$

Here, the maximum stiffness increase occurs when $\frac{h}{b} = 0$, and, again based on table I, the maximum value of D_y/D due to the shell and stringer without fillets equals 1.11. When b equals the stiffener clear height plus the shell thickness h, equation (A8) is identical to equation (36) of reference 24, which is designated therein as an upper bound expression for D_y/D for a shell-stiffener combination without fillets. With b equal to the stiffener clear height plus h from table I, the change in the maximum value of D_y/D is negligible and remains so even when b is arbitrarily reduced to $r_F + h$. Thus, it appears that the value of D_y/D is not particularly affected by wide variations in the choice of $h(y)$ through the stiffener width.

The foregoing procedure could, of course, be used to determine the increase in longitudinal bending stiffness D_x/D in the shell due to closely spaced integral rings.

APPENDIX B

STIFFNESS EXPRESSIONS FOR AN EQUIVALENT-SHELL METHOD OF VIBRATION ANALYSIS

The equivalent-shell frequencies shown in figure 8(b) are based on stiffness expressions given in this appendix which are different from those given in reference 13. The revisions in these expressions for the single-wall shell with stiffeners on one side or the other are due to modifications in the relative stiffnesses assumed to be carried by the shell and the stringer. In reference 13, coupling stiffnesses were assumed to be carried by the shell-stringer combination, and, by virtue of this assumption, together with the equivalent-shell concept, isotropic relations were used to define these stiffnesses, as in reference 29. These isotropic relations have the effect of overestimating the actual stiffness contribution of the shell, particularly in the case of the torsional stiffness.

The correct, more realistic stiffness distribution between stringer and shell is assumed in the following expressions and is based, in part, on the work of Flügge in reference 10:

$$\left.\begin{aligned} D_{12} &= \frac{\mu E_c h_c^3}{12(1-\mu^2)} & \qquad C_{12} &= \frac{\mu E_c h_c}{1-\mu^2} \\ D_{66} &= \frac{E_c h_c^3}{6(1+\mu)} + \frac{G_s J_s}{d} & \qquad C_{66} &= \frac{E_c h_c}{2(1+\mu)} \end{aligned}\right\} \tag{B1}$$

where, as defined in reference 13, D_{12} is the coupled bending stiffness, C_{12} is the coupled stretching stiffness, D_{66} is the torsional stiffness, and C_{66} is the middle-surface shear stiffness. Note that the coupling stiffnesses and middle-surface shear stiffness are now carried by the shell alone, whereas torsion is carried by both shell and stringer but is based on a linear combination of the isotropic shell relation and the beam relation for the stringer.

The remaining stiffnesses in reference 13 (i.e., D_{11}, C_{11}, D_{22}, and C_{22}) are unchanged by these revisions for a single-wall shell with stiffeners either on the inside or outside.

REFERENCES

1. Anon.: Theoretical and Experimental Analysis of Orthotropic-Shell Stability. LMSC-A701014, Lockheed Missiles & Space Co., Sept. 11, 1964.

2. Card, Michael F.: Preliminary Results of Compression Tests on Cylinders With Eccentric Longitudinal Stiffeners. NASA TM X-1004, 1964.

3. Hedgepeth, John M.; and Hall, David B.: Stability of Stiffened Cylinders. AIAA J., vol. 3, no. 12, Dec. 1965, pp. 2275-2286.

4. Block, David L.; Card, Michael F.; and Mikulas, Martin M., Jr.: Buckling of Eccentrically Stiffened Orthotropic Cylinders. NASA TN D-2960, 1965.

5. Mikulas, Martin M., Jr.; and McElman, John A.: On Free Vibrations of Eccentrically Stiffened Cylindrical Shells and Flat Plates. NASA TN D-3010, 1965.

6. McElman, John A.: Eccentrically Stiffened Shallow Shells. Ph. D. Thesis, Virginia Polytech. Inst., 1966.

7. Bushnell, David: Symmetric and Nonsymmetric Buckling of Finitely Deformed Eccentrically Stiffened Shells of Revolution. AIAA J., vol. 5, no. 8, Aug. 1967, pp. 1455-1462.

8. Egle, D. M.; and Sewall, J. L.: An Analysis of Free Vibration of Orthogonally Stiffened Cylindrical Shells With Stiffeners Treated as Discrete Elements. AIAA J., vol. 6, no. 3, Mar. 1968, pp. 518-526.

9. Resnick, Barry S.; and Dugundji, John: Effects of Orthotropicity, Boundary Conditions, and Eccentricity on the Vibrations of Cylindrical Shells. Sci. Rep. AFOSR 66-2821, U.S. Air Force, Nov. 1966. (Available from DDC as AD 648077.)

10. Flügge, Wilhelm: Stresses in Shells. Second printing, Springer-Verlag (Berlin), 1962, pp. 304-306.

11. Baruch, M.; and Singer, J.: Effect of Eccentricity of Stiffeners on the General Instability of Stiffened Cylindrical Shells Under Hydrostatic Pressure. J. Mech. Eng. Sci., vol. 5, no. 1, 1963, pp. 23-27.

12. Baruch, M.: Equilibrium and Stability Equations for Stiffened Shells. Israel J. Technol., vol. 2, no. 1, 1964, pp. 117-124.

13. Sewall, John L.; Clary, Robert R.; and Leadbetter, Sumner A.: An Experimental and Analytical Vibration Study of a Ring-Stiffened Cylindrical Shell Structure With Various Support Conditions. NASA TN D-2398, 1964.

14. Weingarten, V. I.: Free Vibrations of Ring-Stiffened Conical Shells. AIAA J., vol. 3, no. 8, Aug. 1965, pp. 1475-1481.

15. Schnell, Walter; and Heinrichsbauer, Franz-Josef: Zur Bestimmung der Eigenschwingungen Längsversteifter, Dünnwandiger Kreiszylinderschalen. Jahrb. 1963 WGLR, Friedr. Vieweg & Sohn (Braunschweig), pp. 278-286.

16. Hoppmann, W. H., II: Flexural Vibrations of Orthogonally Stiffened Cylindrical Shells. Tech. Rep. No. 11 (Contract Nonr-248(12)), Dep. Mech. Eng., Johns Hopkins Univ., July 1956.

17. Herr, Robert W.: A Wide-Frequency-Range Air-Jet Shaker. NACA TN 4060, 1957.

18. Watkins, Jerry D.; and Clary, Robert R.: Vibrational Characteristics of Some Thin-Walled Cylindrical and Conical Frustum Shells. NASA TN D-2729, 1965.

19. Mixson, John S.: Experimental Modes of Vibration of 14° Conical-Frustum Shells With Free Ends. NASA TN D-4428, 1968.

20. Naumann, Eugene C.; and Flagge, Bruce: A Noncontacting Displacement Measuring Technique and Its Application to Current Vibration Testing. Preprint No. 16.18-5-66, Instrum. Soc. Amer., Oct. 1966.

21. Bishop, R. E. D.; and Johnson, D. C.: The Mechanics of Vibration. Cambridge Univ. Press, 1960, pp. 375-387.

22. Tobias, S. A.: A Theory of Imperfection for the Vibrations of Elastic Bodies of Revolution. Engineering, vol. 172, no. 4470, Sept. 28, 1951, pp. 409-410.

23. Novozhilov, V. V. (P. G. Lowe, trans.): The Theory of Thin Shells. P. Noordhoff Ltd. (Groningen, The Netherlands), 1959, pp. 24, 188.

24. Huffington, Norris J., Jr.; Schumacher, Robert N.; and Irwin, Ruth L.: Bending Athwart a Parallel-Stiffened Plate. RR-53, Martin Co., Dec. 1964.

25. Arnold, R. N.; and Warburton, G. B.: The Flexural Vibrations of Thin Cylinders. Proc. (A) Inst. Mech. Eng. (London), vol. 167, no. 1, 1953, pp. 62-74.

26. Warburton, G. B.: Vibration of Thin Cylindrical Shells. J. Mech. Eng. Sci., vol. 7, no. 4, Dec. 1965, pp. 399-407.

27. Felgar, Robert P., Jr.: Formulas for Integrals Containing Characteristic Functions of a Vibrating Beam. Circ. No. 14, Bur. Eng. Res., Univ. of Texas, 1950.

28. Arnold, R. N.; and Warburton, G. B.: Flexural Vibrations of the Walls of Thin Cylindrical Shells Having Freely Supported Ends. Proc. Roy. Soc. (London), ser. A, vol. 197, no. 1049, June 7, 1949, pp. 238-256.

29. Nelson, H. C.; Zapotowski, B.; and Bernstein, M.: Vibration Analysis of Orthogonally Stiffened Circular Fuselage and Comparison With Experiment. Proceedings of the National Specialists Meeting on Dynamics and Aeroelasticity, Inst. Aeronaut. Sci., Nov. 1958, pp. 77-87.

TABLE I.- GEOMETRICAL AND STRUCTURAL PROPERTIES OF MODELS

[Stiffener dimensions averaged from 60 discrete measurements]

Property	Model		
	Internally stiffened	Unstiffened	Externally stiffened
Radius to shell middle surface, R	9.535 in. (242.2 mm)	9.538 in. (242.3 mm)	9.537 in. (242.2 mm)
Shell thickness, h	0.0266 in. (0.676 mm)	0.0255 in. (0.648 mm)	0.0256 in. (0.650 mm)
Fillet radius, r_F	1/16 in. (1.588 mm)	----------	1/16 in. (1.588 mm)
Stiffener width, $2r_S$	0.100 in. (2.540 mm)	----------	0.100 in. (2.540 mm)
Stiffener height	0.2754 in. (6.995 mm)	----------	0.2764 in. (7.021 mm)
Stiffener spacing, d	1.00 in. (25.4 mm)	----------	1.00 in. (25.4 mm)
Cylinder length for various end conditions, L:			
Free-free	25.125 in. (63.82 cm)	25.125 in. (63.82 cm)	25.125 in. (63.82 cm)
Clamped-free	24.625 in. (62.55 cm)	24.625 in. (62.55 cm)	24.625 in. (62.55 cm)
Simply supported	24.00 in. (60.96 cm)	24.00 in. (60.96 cm)	24.00 in. (60.96 cm)
Clamped-clamped	24.00 in. (60.96 cm)	24.00 in. (60.96 cm)	24.00 in. (60.96 cm)
Young's modulus for shell and stringers, $E_C = E_S$	10^7 psi (68.95 GN/m^2)	10^7 psi (68.95 GN/m^2)	10^7 psi (68.95 GN/m^2)
Poisson's ratio for shell, μ	0.315	0.315	0.315
Shear modulus for stringers, G_S	3.8×10^6 psi (26.2 GN/m^2)	----------	3.8×10^6 psi (26.2 GN/m^2)
Mass density for shell and stringers, $\rho_C = \rho_S$	2.54×10^{-4} lb-sec^2 (2.7145×10^3 Kg/m^3)	2.54×10^{-4} lb-sec^2 (2.7145×10^3 Kg/m^3)	2.54×10^{-4} lb-sec^2 (2.7145×10^3 Kg/m^3)
Cross-sectional area of stringer, A_S	0.029219 in^2 (18.85 mm^2)	----------	0.029319 in^2 (18.92 mm^2)
Distance from shell middle surface to stringer centroid, $\bar{z}_S$	-0.1438 in. (-3.653 mm)	----------	0.1439 in. (3.655 mm)
Polar moment of inertia of stringer about shell middle surface, J_{e_S}	0.832256×10^{-3} in^4 (0.034641 cm^4)	----------	0.836124×10^{-3} in^4 (0.034802 cm^4)

TABLE II.- RESULTS OF VIBRATION TESTS OF UNSTIFFENED AND ECCENTRICALLY STIFFENED CYLINDRICAL SHELLS WITH SIMPLY SUPPORTED END CONDITIONS

n	Frequency, Hz, for –							
	Unstiffened cylinder			Internally stiffened cylinder			Externally stiffened cylinder	
	m = 1	m = 2	m = 3	m = 1	m = 2	m = 3	m = 1	m = 2
4	287.0	----------	----------	233.0	----------	----------	----------	----------
5	203.0 and 211.0	----------	----------	175.0	----------	----------	231.0	----------
6	175.0	----------	----------	137.0 and 147.0	----------	----------	197.0 and 201.0	----------
7	163.0 and 169.0	----------	----------	142.0 and 150.0	----------	----------	189.0	----------
8	188.0	345.0 and 346.0	----------	169.0	319.0	602.0 and 605.0	199.0	----------
9	224.0	----------	----------	203.0	333.0	----------	219.0	----------
10	268.0	339.0 and 342.0	----------	243.0	366.0	----------	252.0	469.0 and 478.0
11	326.0	369.0 and 370.0	491.0 and 507.0	290.0	399.0	622.0	290.0	489.0
12	382.0 and 385.0	409.0 and 411.0	510.0 and 517.0	333.0	443.0	664.0	336.0	507.0 and 512.0
13	440.0	471.0 and 479.0	----------	392.0	482.0	----------	378.0 and 386.0	546.0
14	----------	----------	604.0	450.0	551.0 and 560.0	761.0	440.0	590.0
15	590.0	----------	----------	502.0	----------	----------	500.0	630.0

TABLE III.- RESULTS OF VIBRATION TESTS OF UNSTIFFENED AND ECCENTRICALLY STIFFENED CYLINDRICAL SHELLS WITH FREE-FREE END CONDITIONS

n	Frequency[1], Hz, for –									
	Unstiffened cylinder				Internally stiffened cylinder			Externally stiffened cylinder		
	m = 0	m = 1	m = 2	m = 3	m = 0	m = 1	m = 2	m = 0	m = 1	m = 2
2	11.8	14.8	----	----	5.0	21.0	----	4.8	20.5	----
	7.2	9.2	----	----	6.1	15.8	----	5.9	15.2	----
3	24.5	26.8	----	----	18.0	35.0	----	17.5	34.5	----
	20.1	22.3	----	----	16.1	31.4	----	15.7	31.1	----
4	40.1	44.6	----	----	32.0	52.0	----	30.8	52.5	----
	37.9	40.3	----	----	30.4	50.4	----	30.6	49.4	----
5	63.4	66.8	367.0	----	51.3	71.0	----	50.0	72.0	----
	61.9	65.0		----	51.1	70.3	----	50.1	69.7	
6	91.7	94.8	292.0	----	74.0	96.0	273.0	71.0	94.0	----
	91.6	94.6			74.0	95.8		71.0	94.0	
7	125.6	129.0	242.0	----	102.0	124.0	245.0	98.0	122.0	----
	125.0	129.0		----	102.0	124.0		98.0	122.0	----
8	165.0	170.0	235.0	----	132.0	158.0	252.0	129.0	159.0	320.0
	165.0	170.0			132.0	158.0		129.0	159.0	
9	210.0	214.0	252.0	----	170.0	195.0	276.0	165.0	189.0	330.0
	210.0	214.0		----	170.0	195.0		165.0	189.0	
10	262.0	266.0	290.0	----	210.0	234.0	312.0	208.0	232.0	352.0
	262.0	266.0			210.0	234.0		208.0	232.0	
11	318.0	322.0	339.0	----	255.0	280.0	358.0	249.0	273.0	388.0
	318.0	322.0			255.0	280.0		249.0	273.0	
12	378.0	382.0	----	----	302.0	330.0	405.0	295.0	318.0	422.0
	378.0	382.0			302.0	330.0		295.0	318.0	
13	443.0	452.0	459.0	501.0	351.0	382.0	455.0	348.0	----	470.0
	443.0	452.0			351.0	382.0		348.0		
14	512.0	521.0	533.0	564.0	410.0	----	----	403.0	430.0	----
	512.0	521.0			410.0			403.0	430.0	
15	----	----	----	----	----	----	----	----	493.0	----
									493.0	

[1]In each group, the first value given was obtained with the electrodynamic shaker and the second value, with the air shaker.

TABLE IV.- RESULTS OF VIBRATION TESTS OF UNSTIFFENED AND ECCENTRICALLY STIFFENED CYLINDRICAL SHELLS WITH CLAMPED-CLAMPED END CONDITIONS

n	Frequency, Hz, for –							
	Unstiffened cylinder			Internally stiffened cylinder			Externally stiffened cylinder	
	m = 1	m = 2	m = 3	m = 1	m = 2	m = 3	m = 1	m = 2
4	----------	----------	----	356.0	----	----------	----	----
5	321.0 and 325.0	----------	----	275.0	----	----------	347.0	----
6	263.0	----------	----	228.0	----	----------	313.0	----
7	233.0	479.0	----	207.0	449.0	----------	282.0	----
8	227.0	418.0 and 423.0	----	212.0	423.0	----------	272.0	----
9	244.0	----------	----	231.0	418.0	----------	287.0	----
10	281.0	----------	583.0	262.0	435.0	----------	305.0	578.0
11	----------	397.0 and 404.0	562.0	302.0 and 308.0	467.0	----------	333.0	----
12	386.0	----------	----	356.0	----	757.0 and 763.0	370.0	605.0
13	453.0	490.0	----	405.0	551.0	803.0	----	630.0
14	515.0	552.0	----	457.0	603.0	846.0	466.0	----
15	----------	622.0	690.0	522.0	660.0	----------	525.0	711.0

TABLE V.- RESULTS OF VIBRATION TESTS OF UNSTIFFENED AND ECCENTRICALLY STIFFENED CYLINDRICAL SHELLS WITH CLAMPED-FREE END CONDITIONS

n	Frequency, Hz, for –							
	Unstiffened cylinder			Internally stiffened cylinder			Externally stiffened cylinder	
	m = 1	m = 2	m = 3	m = 1	m = 2	m = 3	m = 1	m = 2
2	----------	----------	----------	----------	----------	----	277.0	----------
3	155.0 and 157.0	----------	----------	147.0	----------	----	161.0 and 166.0	----------
4	107.0	----------	----------	99.0	390.0	----	110.0 and 114.0	473.0
5	89.0 and 91.0	341.0	----------	80.0 and 83.0	303.0	----	94.0 and 97.0	377.0
6	102.0	276.0	----------	90.0 and 93.0	247.0	544.0	100.0	340.0
7	130.0	240.0	----------	113.0	225.0	----	121.0	308.0 and 310.0
8	166.0	227.0 and 231.0	----------	143.0	233.0	----	147.0	298.0 and 301.0
9	208.0	246.0	400.0	177.0	257.0	434.0	181.0	----------
10	260.0	281.0	----------	217.0	290.0 and 295.0	456.0	217.0 and 222.0	328.0 and 330.0
11	317.0	337.0	409.0 and 412.0	267.0	331.0	491.0	259.0	365.0
12	374.0	393.0 and 396.0	----------	312.0	384.0	524.0	316.0	----------
13	----------	455.0 and 461.0	476.0	363.0	438.0	584.0	360.0	444.0
14	523.0	531.0	558.0	425.0	494.0	627.0	418.0	----------
15	----------	603.0	633.0	486.0	535.0	----	495.0	544.0

TABLE VI.- LONGITUDINAL MODAL PROPERTIES BASED ON BEAM FUNCTIONS

(a) Functions and integrals (from ref. 27, except for simply supported end condition and free-free end condition for m = 0 and 1)

Function or integral	End condition: Free-free, m = 0	Free-free, m = 1	Free-free, m ≥ 2	Clamped-free, m ≥ 1	Clamped-clamped, m ≥ 1	Simply supported, m ≥ 1	
$X_m(x)$	1	$\frac{x}{L} - \frac{1}{2}$	$\cosh N_m x + \cos N_m x - \gamma_m(\sinh N_m x + \sin N_m x)$	$\cosh N_m x - \cos N_m x - \gamma_m(\sinh N_m x - \sin N_m x)$	$\cosh N_m x - \cos N_m x - \gamma_m(\sinh N_m x - \sin N_m x)$	$\sin \frac{m\pi x}{L}$	
$I_1 = \int_0^L X_i X_m \, dx$	L	L/12	L	L	L	L/2	i = m
	0	0	0	0	0	0	i ≠ m
$I_2 = \int_0^L X_i' X_m' \, dx$	0	$\frac{1}{L}$	$\gamma_m N_m(\gamma_m N_m L + 6)$	$\gamma_m N_m(\gamma_m N_m L + 2)$	$\gamma_m N_m(\gamma_m N_m L - 2)$	$\frac{(m\pi)^2}{2L}$	i = m
	0	0	$\frac{4N_i N_m(\gamma_i N_m^3 - \gamma_m N_i^3)}{N_m^4 - N_i^4}\left[1 + (-1)^{i+m}\right]$	$\frac{4N_i N_m}{N_m^4 - N_i^4}\left[(-1)^{i+m}(\gamma_m N_i^3 - \gamma_i N_m^3) - N_i N_m(\gamma_i N_i - \gamma_m N_m)\right]$	$\frac{4N_i^2 N_m^2(\gamma_i N_i - \gamma_m N_m)}{N_m^4 - N_i^4}\left[1 + (-1)^{i+m}\right]$	0	i ≠ m
$I_3 = \int_0^L X_i'' X_m'' \, dx$	0	0	$N_m^4 L$	$N_m^4 L$	$N_m^4 L$	$\frac{(m\pi)^4}{2L^3}$	i = m
	0	0	0	0	0	0	i ≠ m
$I_{41} = \int_0^L X_i'' X_m \, dx$*	0	0	$-\gamma_m N_m(\gamma_m N_m L - 2)$	$-\gamma_m N_m(\gamma_m N_m L - 2)$	$-\gamma_m N_m(\gamma_m N_m L - 2)$	$-\frac{(m\pi)^2}{2L}$	i = m
	0	0	$\frac{4N_i^4(\gamma_m N_m - \gamma_i N_i)}{N_m^4 - N_i^4}\left[1 + (-1)^{i+m}\right]$	$\frac{4N_i^2(\gamma_m N_m - \gamma_i N_i)}{N_m^4 - N_i^4}\left[(-1)^{i+m} N_i^2 + N_m^2\right]$	$-\frac{4N_i^2 N_m^2(\gamma_i N_i - \gamma_m N_m)}{N_m^4 - N_i^4}\left[1 + (-1)^{i+m}\right]$	0	i ≠ m

*$I_{42} = \int_0^L X_i X_m'' \, dx$.

(b) Values of eigenvalue parameters N_m and γ_m (from ref. 21)

m: Clamped ends	m: Free ends	$N_m L$	γ_m	Clamped-free ends: m	$N_m L$	γ_m
1	2	4.73004	0.9825022	1	1.87510	0.7340955
2	3	7.85320	1.0007773	2	4.69409	1.0184664
3	4	10.9956	.9999665	3	7.85476	.9992245
4	5	14.1372	1.0000015	4	10.9955	1.0000336
5	6	17.2788	.9999999	5	14.1372	.9999986
>5	---	$(2m + 1)\frac{\pi}{2}$	1	>5	$(2m - 1)\frac{\pi}{2}$	1
---	>6	$(2m - 1)\frac{\pi}{2}$	1			

Equations for $N_m L$ and γ_m

$\cosh N_m L \cos N_m L = 1$	$\cosh N_m L \cos N_m L = -1$
$\gamma_m = \frac{\cosh N_m L - \cos N_m L}{\sinh N_m L - \sin N_m L}$	$\gamma_m = \frac{\sinh N_m L - \sin N_m L}{\cosh N_m L + \cos N_m L}$

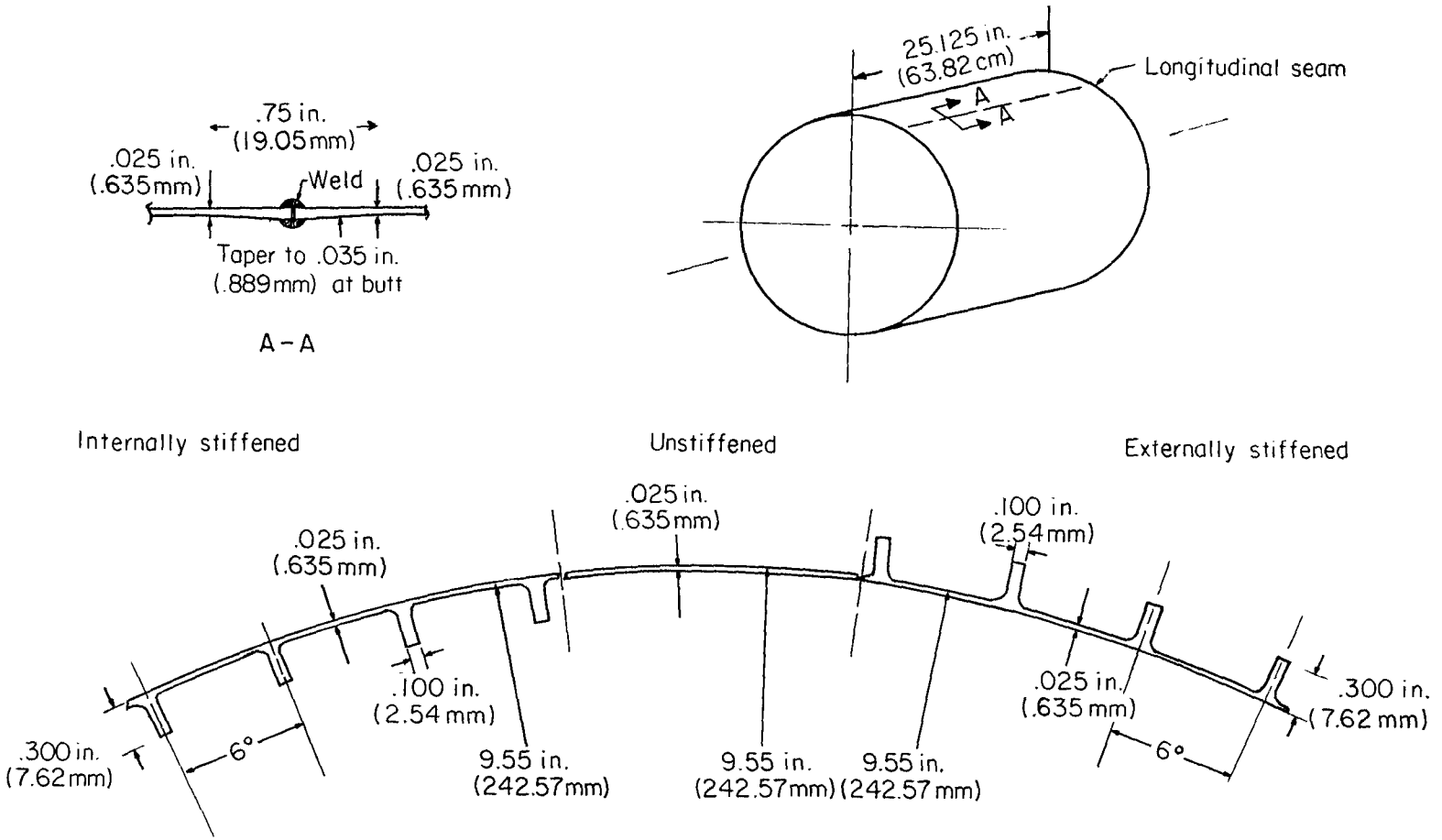

Figure 1.- Geometrical and structural details of models. Dimensions are nominal.

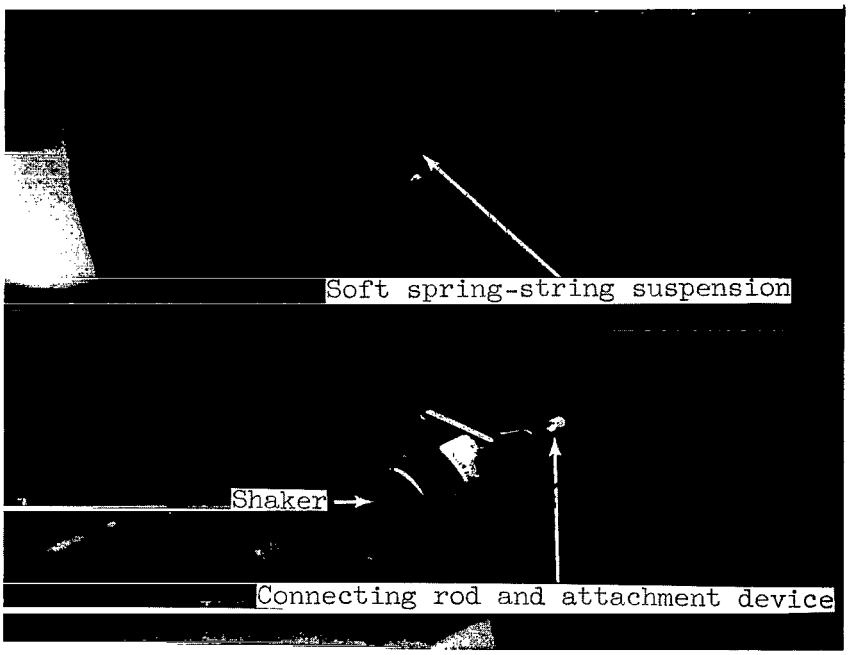

(a) Vacuum-cup fastener.

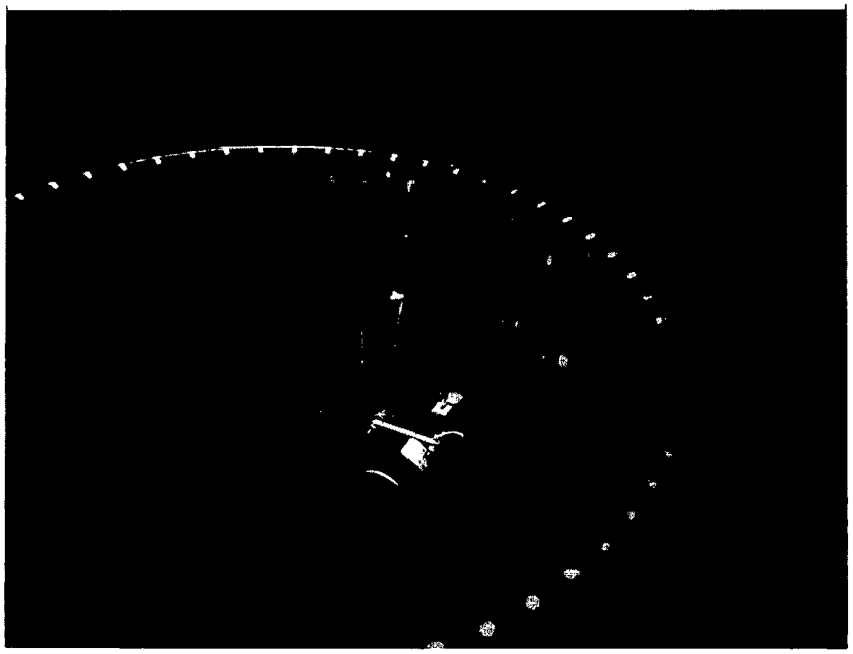

(b) Mechanical fastener.

Figure 2.- Pictorial views of shaker installations.

L-68-893

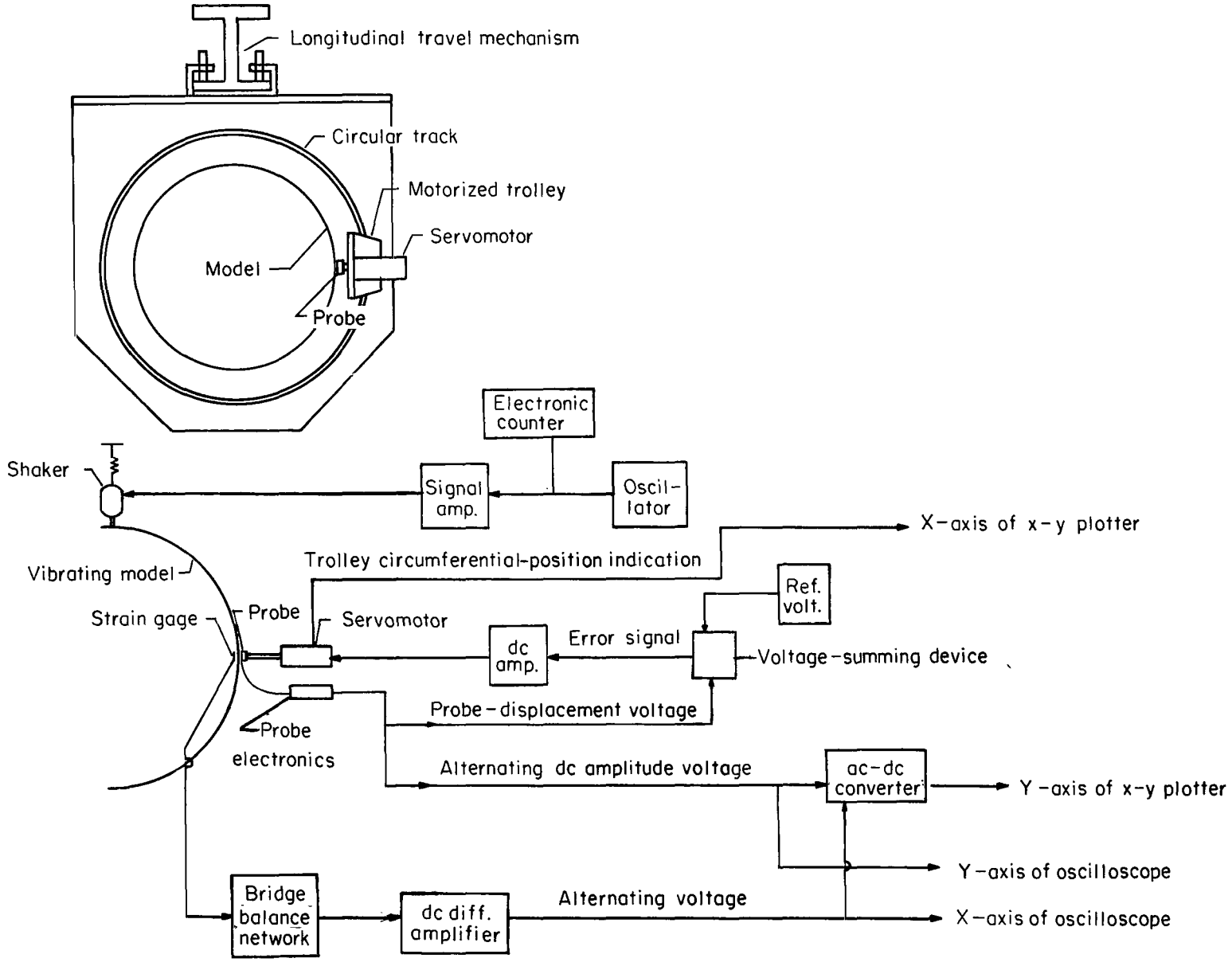

Figure 3.- Instrumentation.

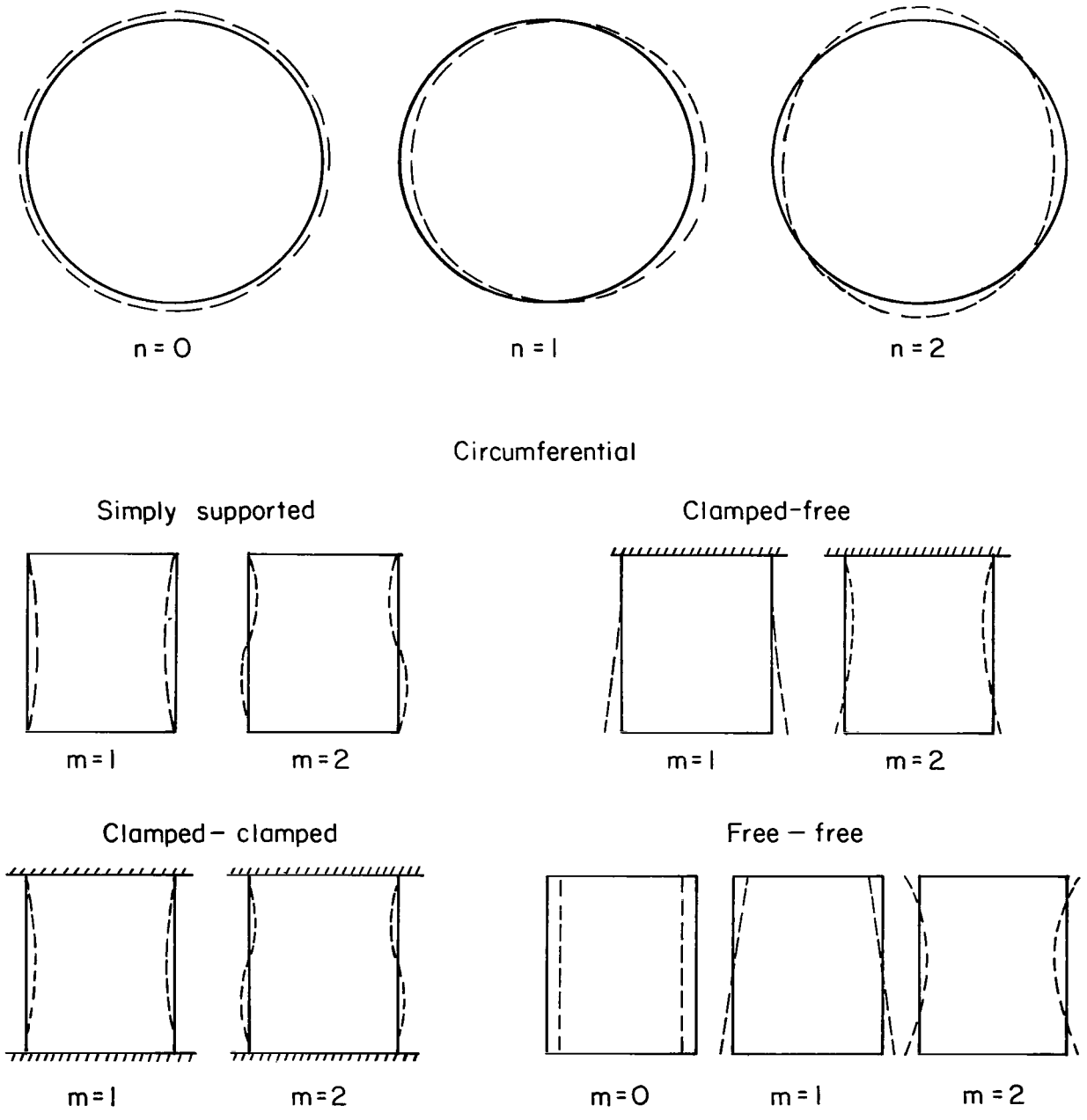

Figure 4.- Identification of circumferential and longitudinal radial mode shapes of cylindrical shells.

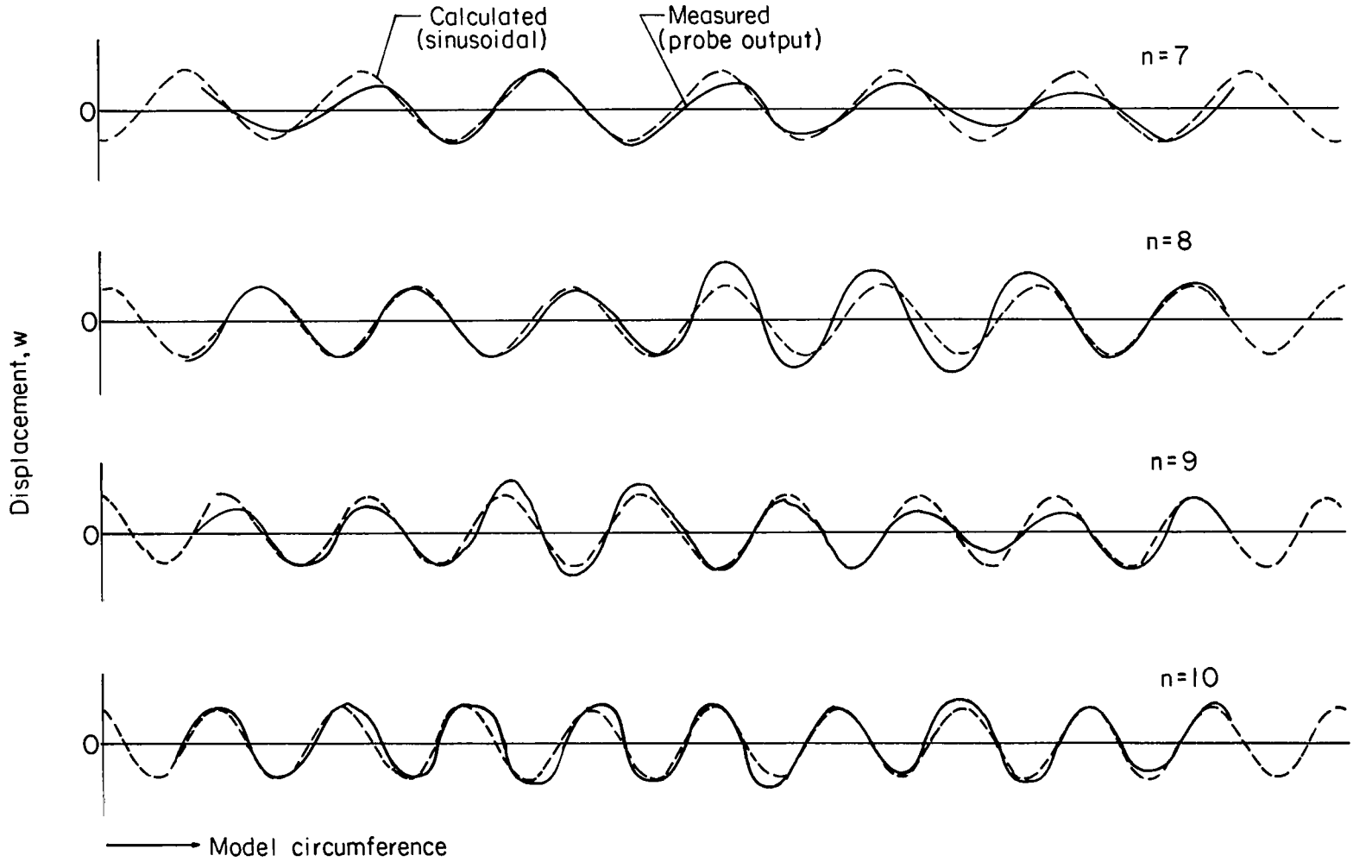

(a) Circumferential mode shapes. Clamped-free internally stiffened shell; m = 1.

Figure 5.- Typical experimental and analytical mode-shape data.

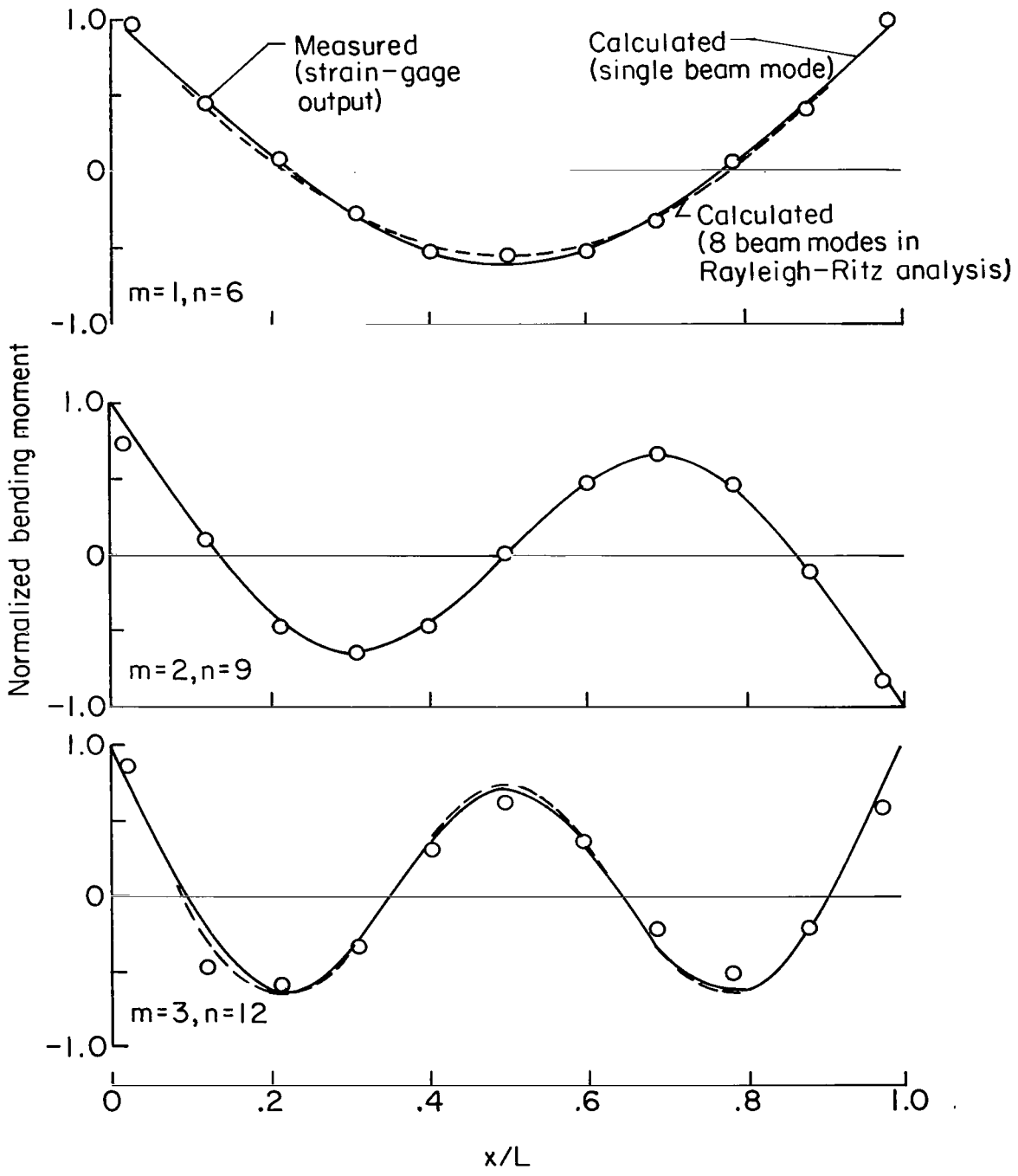

(b) Longitudinal moment distributions for clamped-clamped internally stiffened shell.

Figure 5.- Concluded.

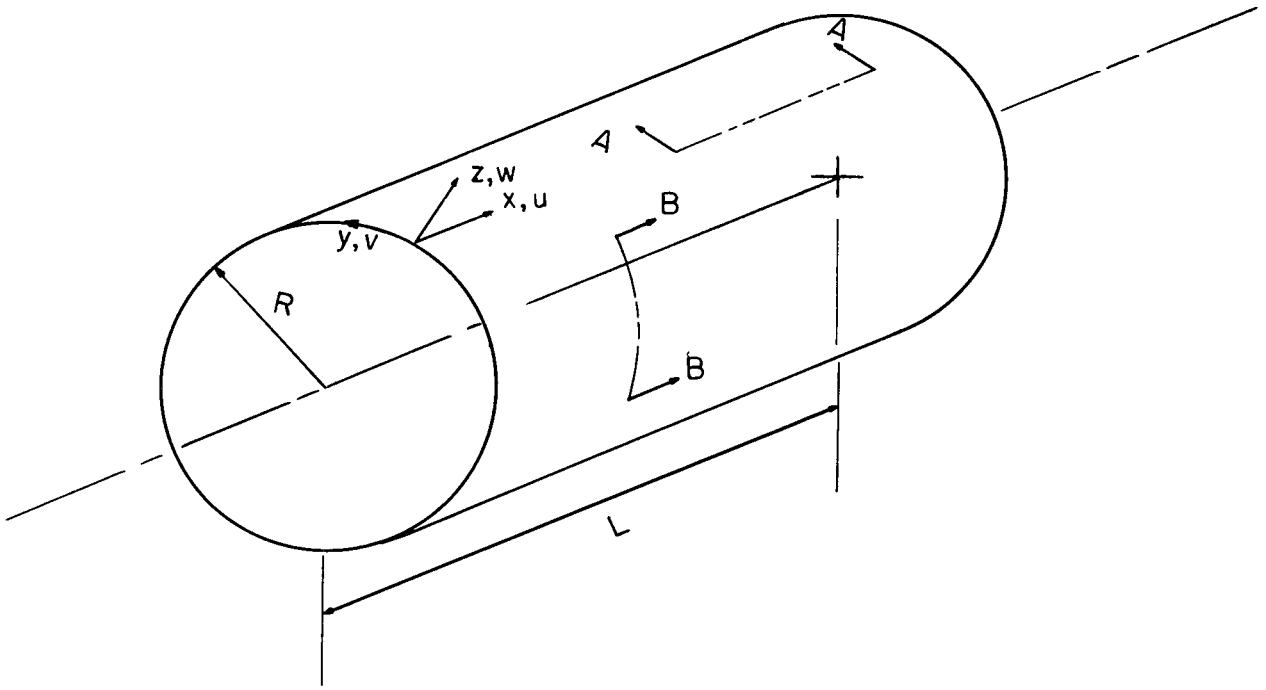

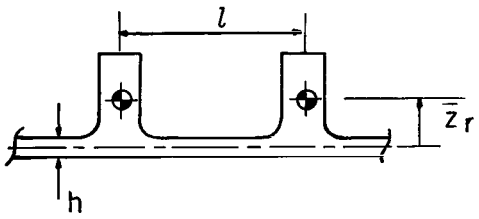

Ring detail

A-A

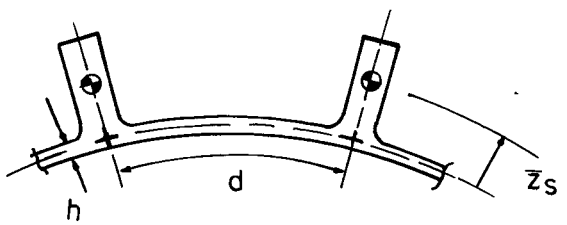

Stringer detail

B-B

Figure 6.- Mathematical model of eccentrically stiffened cylindrical shell with closely spaced rings and stringers.

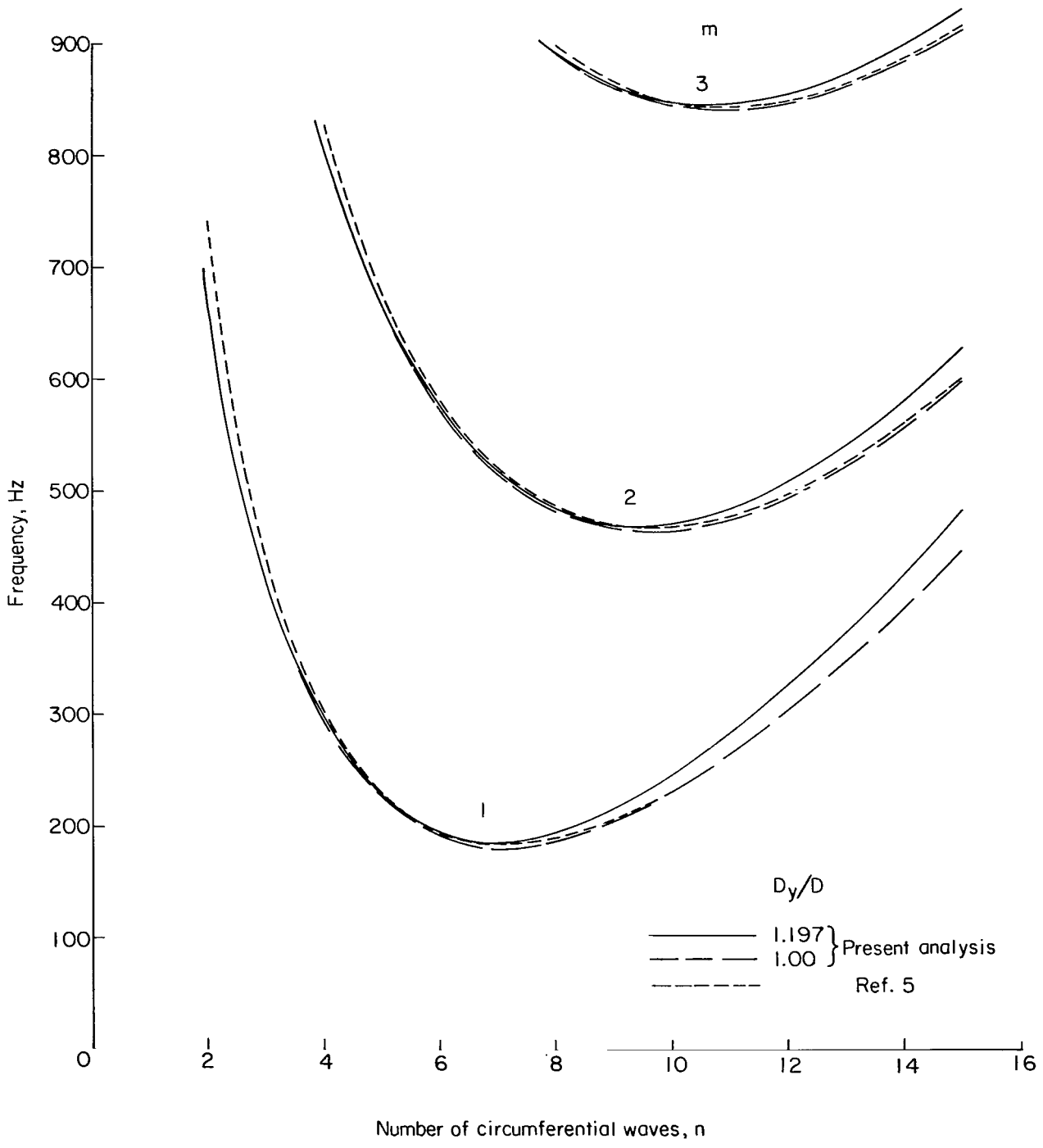

(a) Effects of local circumferential bending stiffness. Simply supported shell.

Figure 7.- Effects of various features of analysis on calculated frequencies of externally stiffened shell.

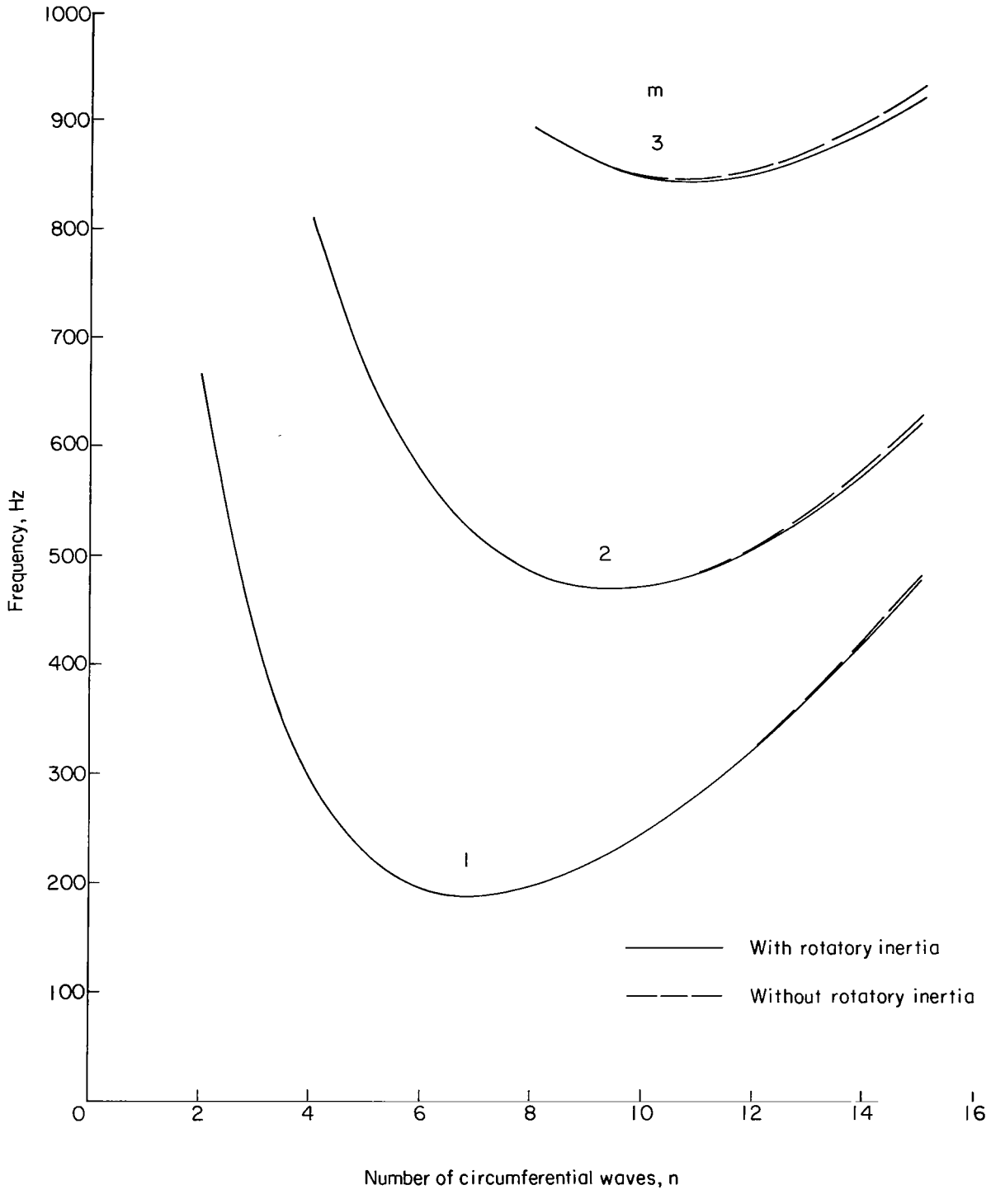

(b) Effects of rotatory inertia of stiffeners. Simply supported shell; $D_y/D = 1.197$.

Figure 7.- Continued.

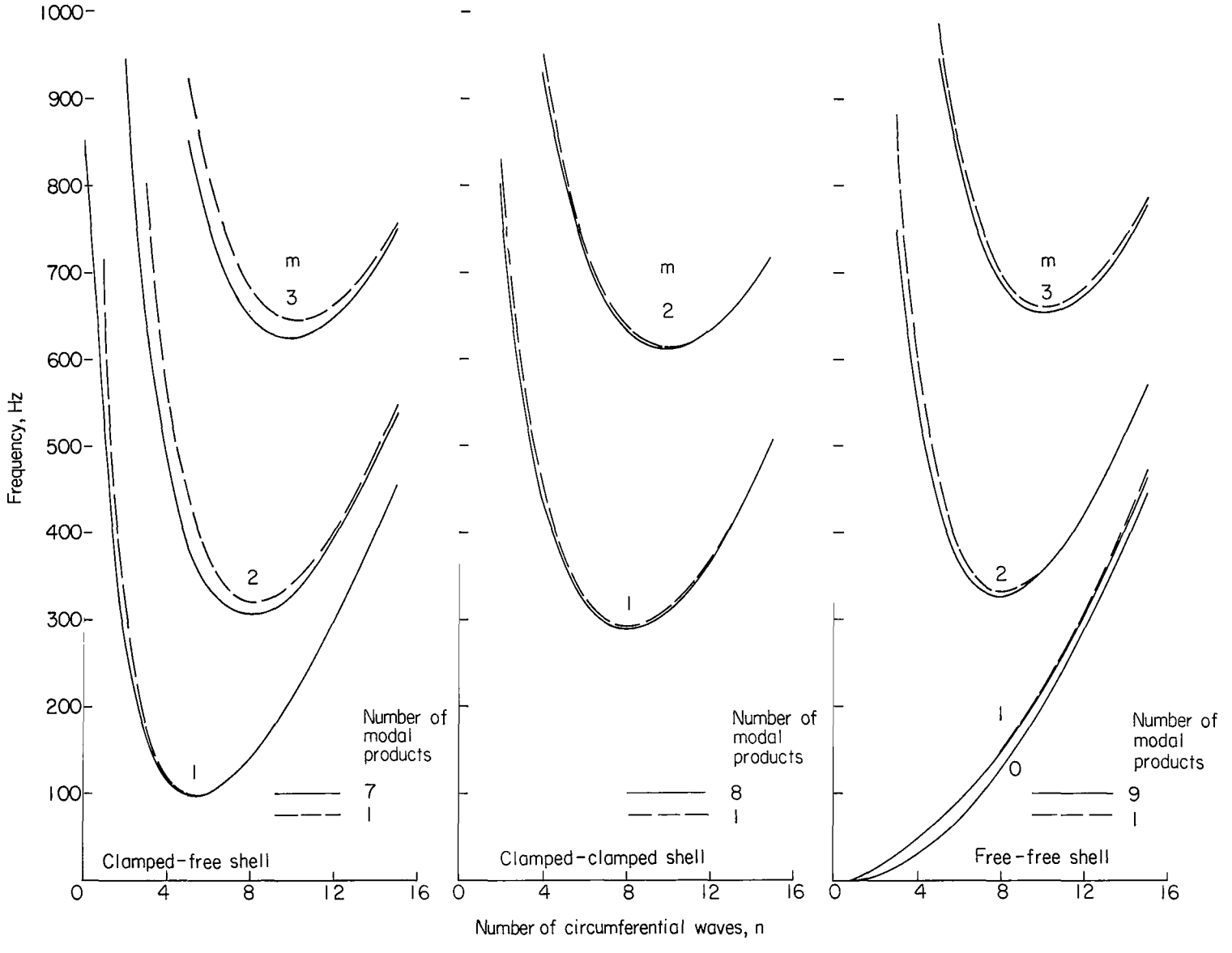

(c) Effects of modal coupling. $D_y/D = 1.197$; rotatory inertia included.

Figure 7.- Concluded.

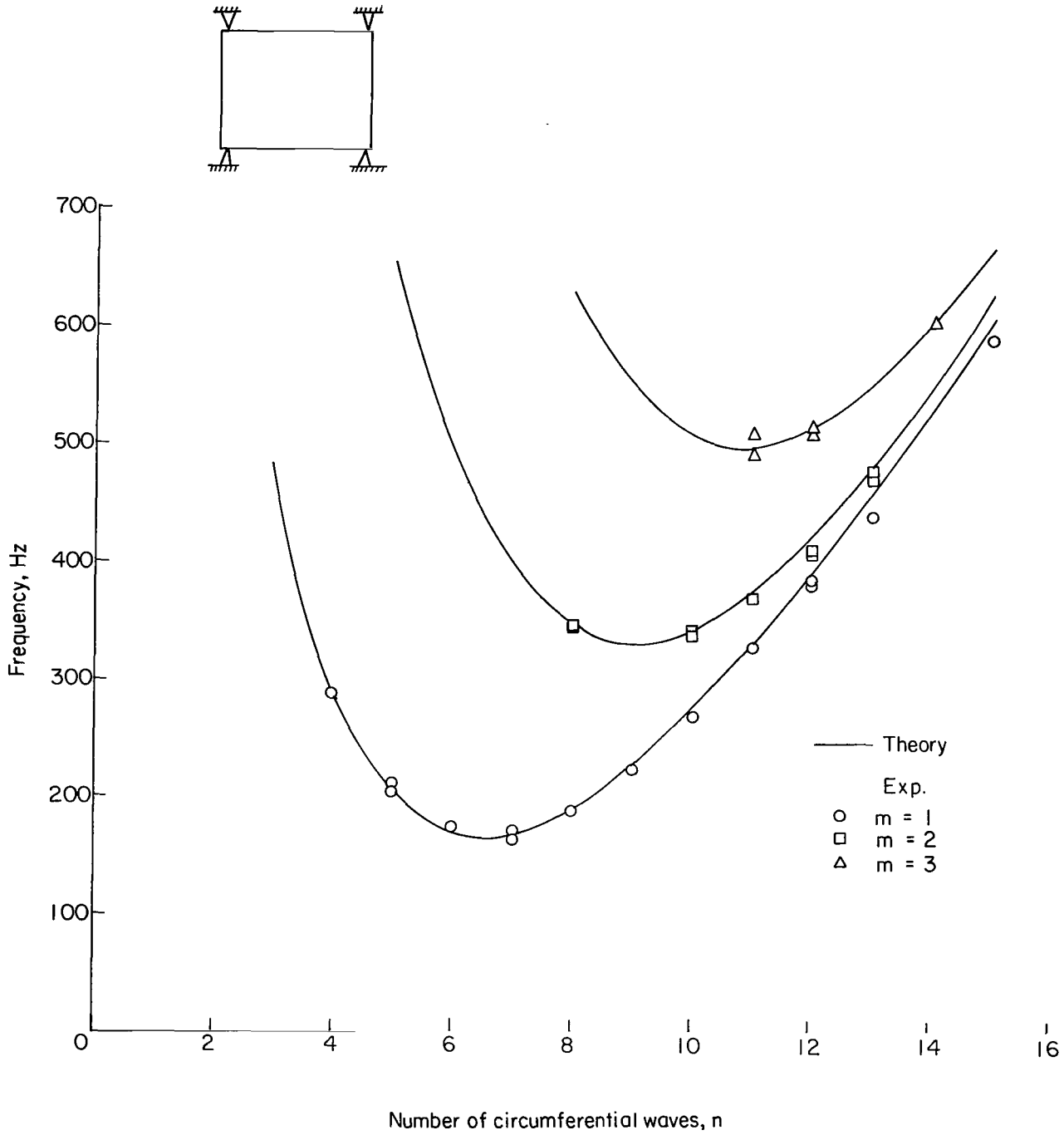

(a) Unstiffened shell.

Figure 8.- Experimental and analytical frequencies of simply supported cylindrical shells.

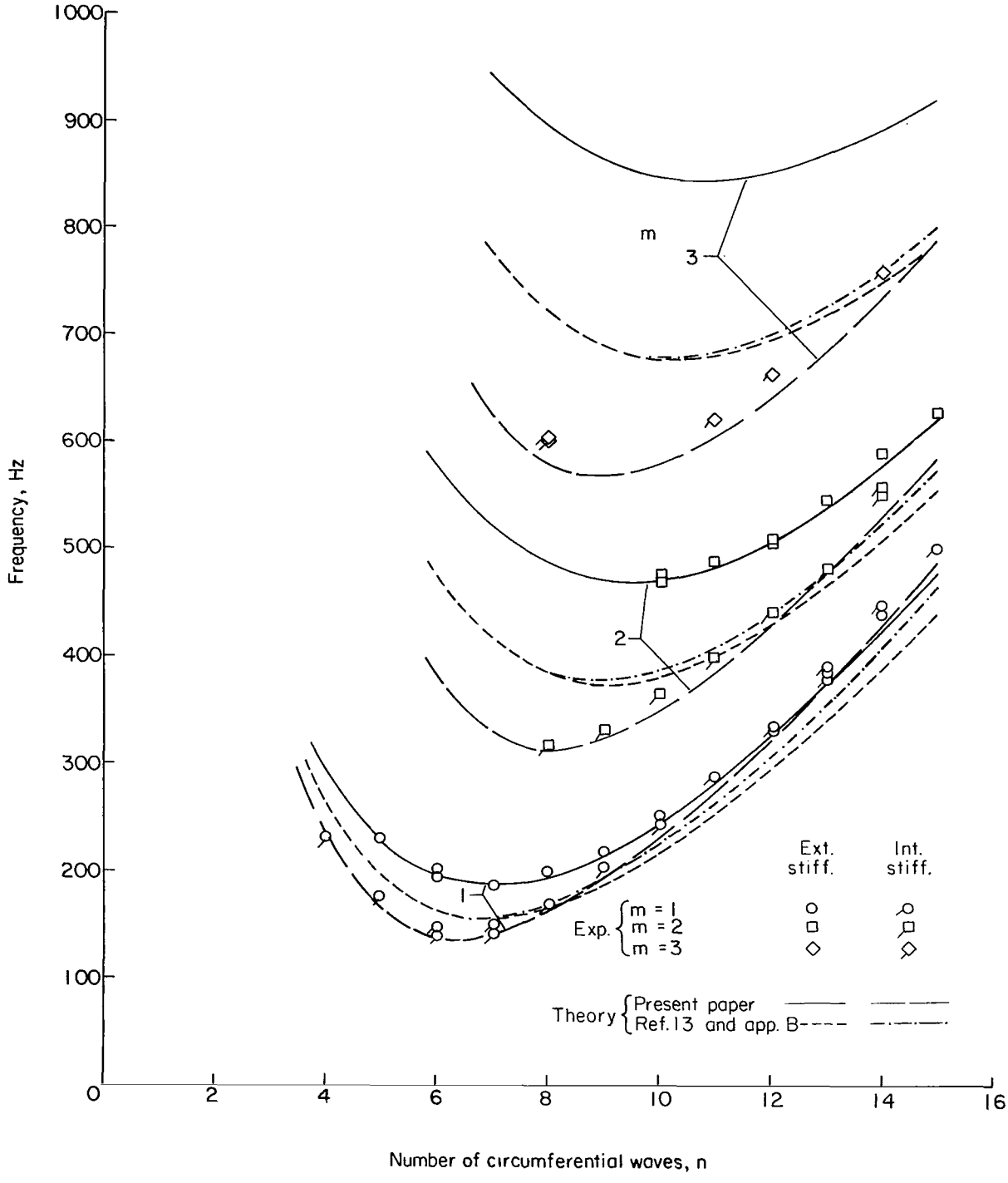

(b) Externally and internally stiffened shells.

Figure 8.- Concluded.

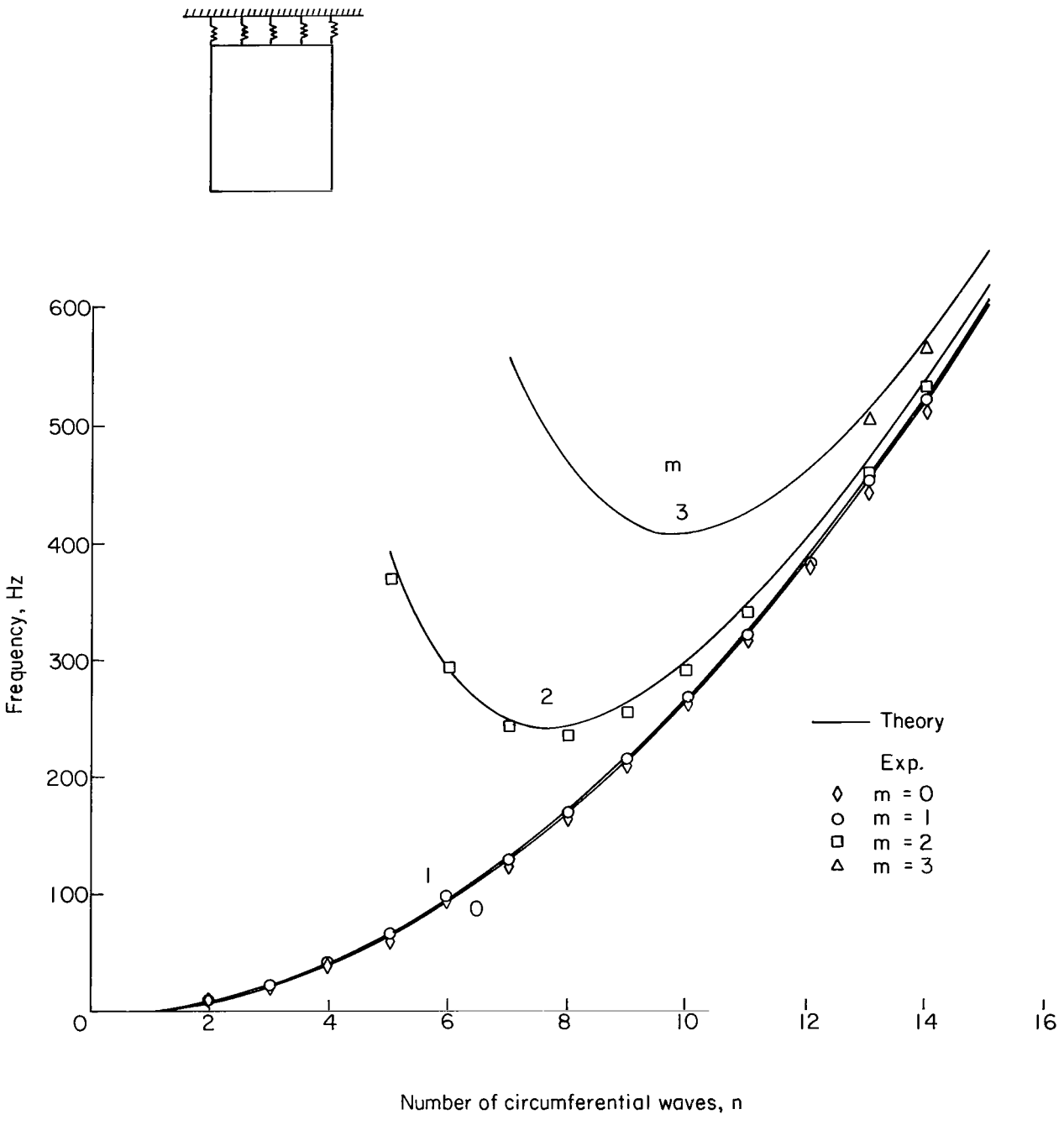

(a) Unstiffened shell.

Figure 9.- Experimental and analytical frequencies of free-free cylindrical shells.

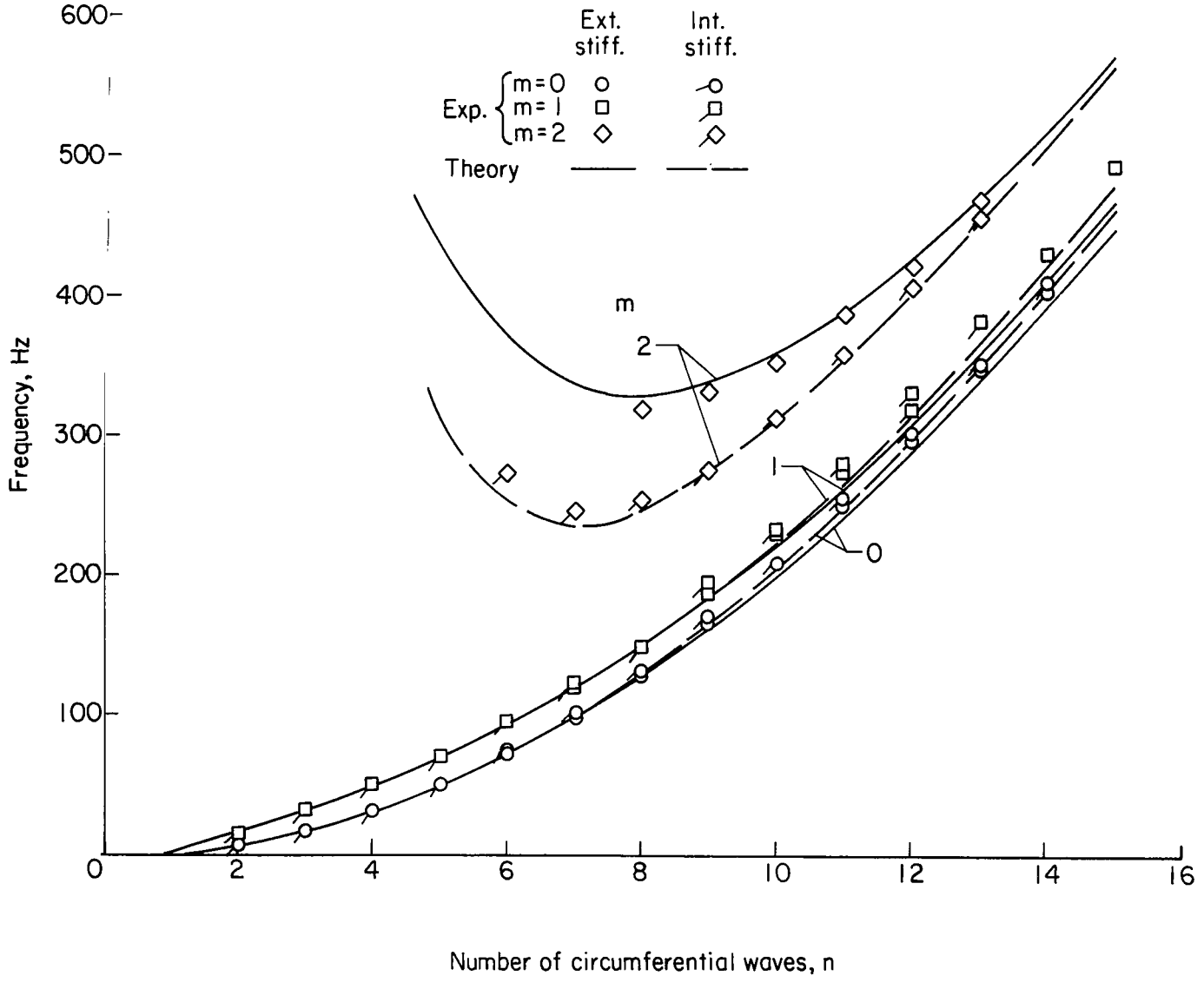

(b) Externally and internally stiffened shells.

Figure 9.- Concluded.

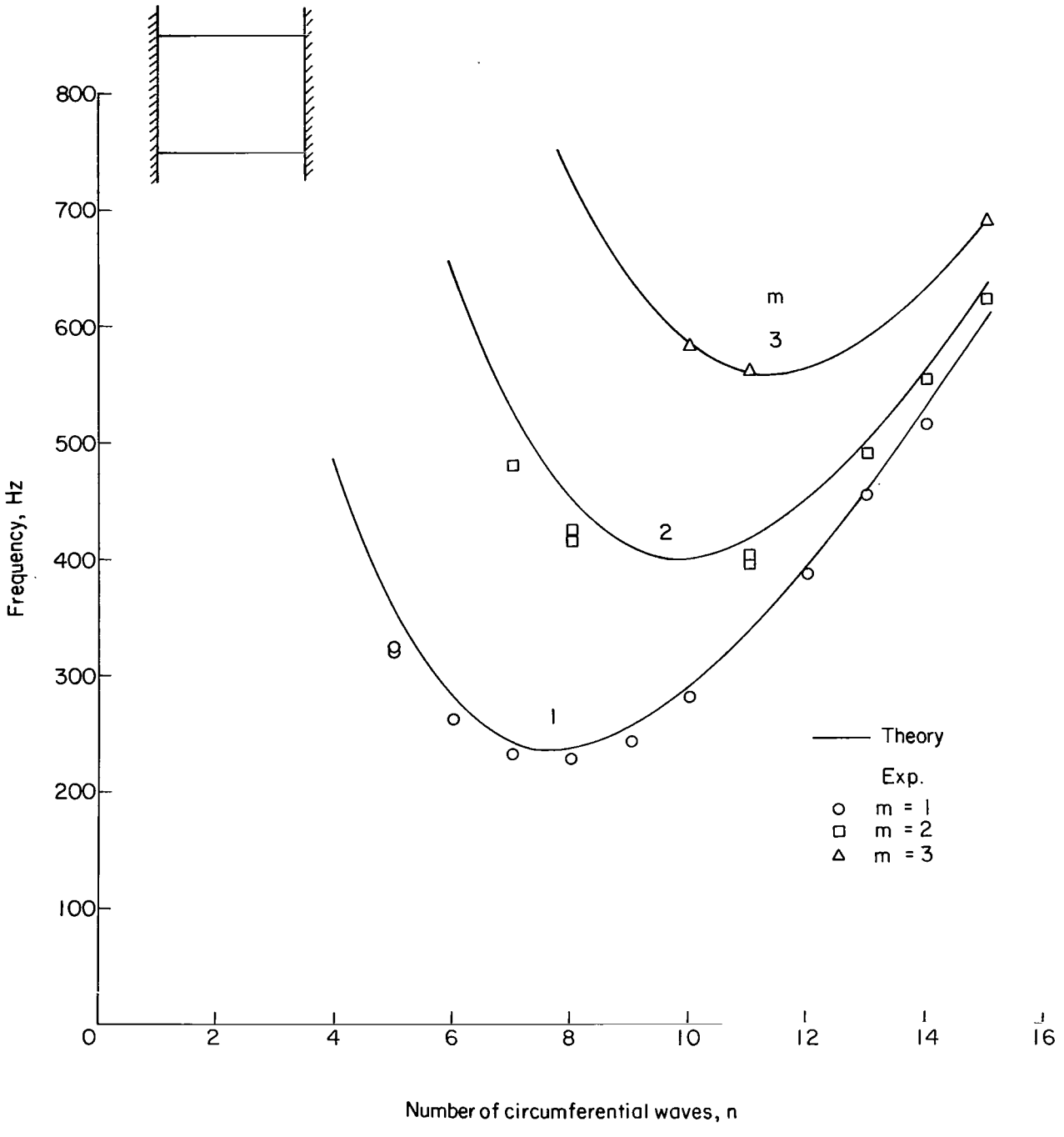

(a) Unstiffened shell.

Figure 10.- Experimental and analytical frequencies of clamped-clamped cylindrical shells.

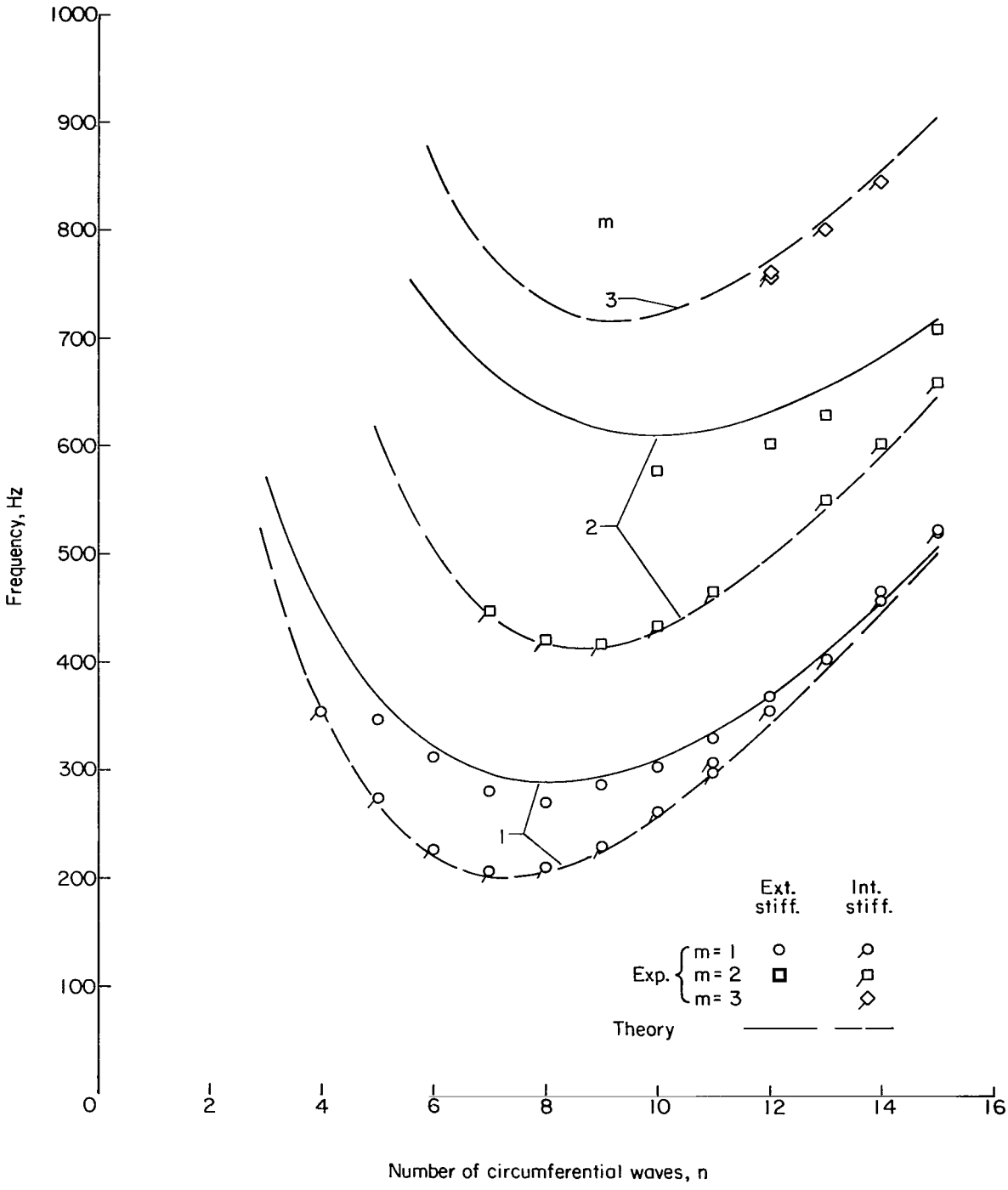

(b) Externally and internally stiffened shells.

Figure 10.- Concluded.

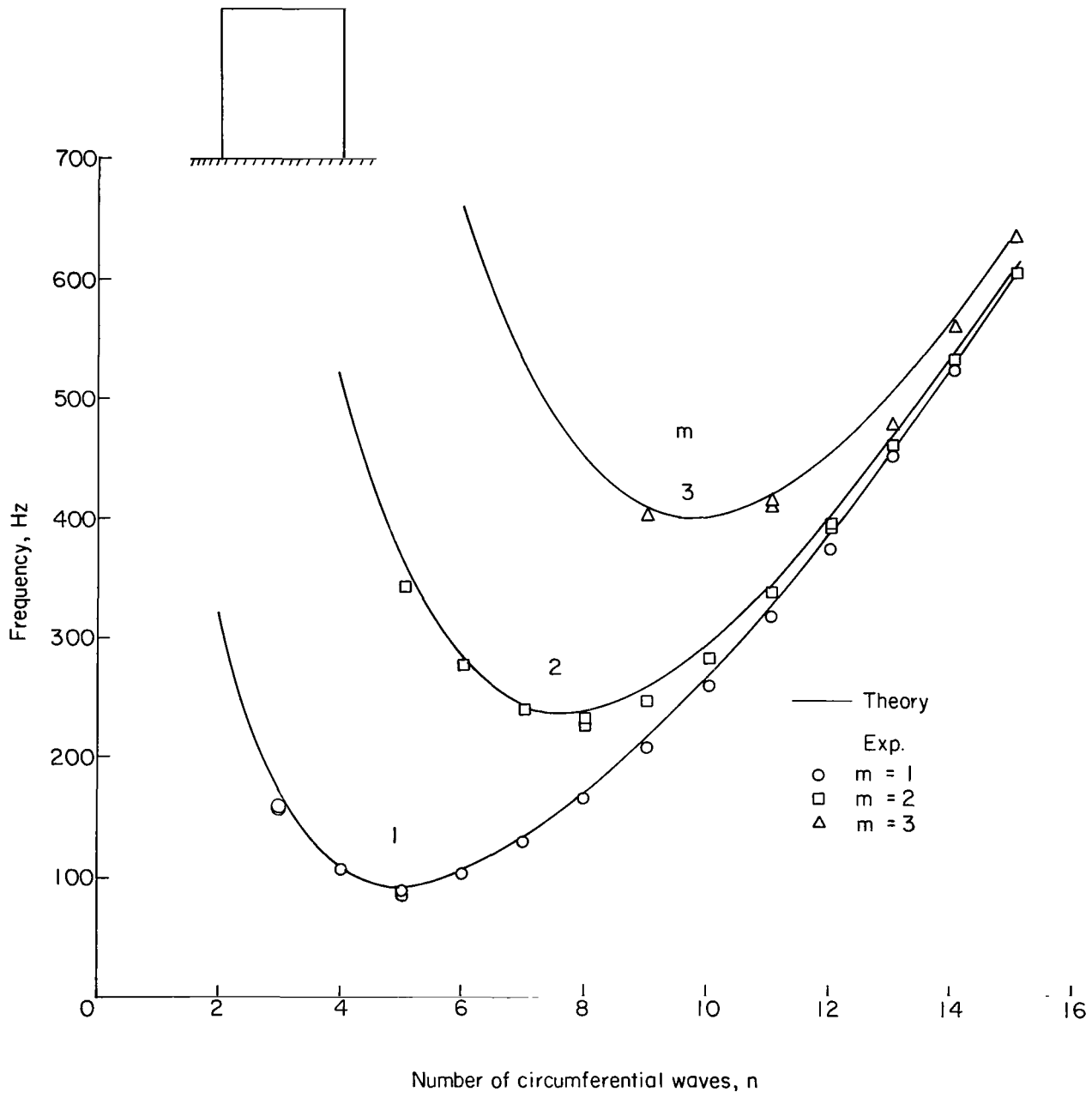

(a) Unstiffened shell.

Figure 11.- Experimental and analytical frequencies of clamped-free cylindrical shells.

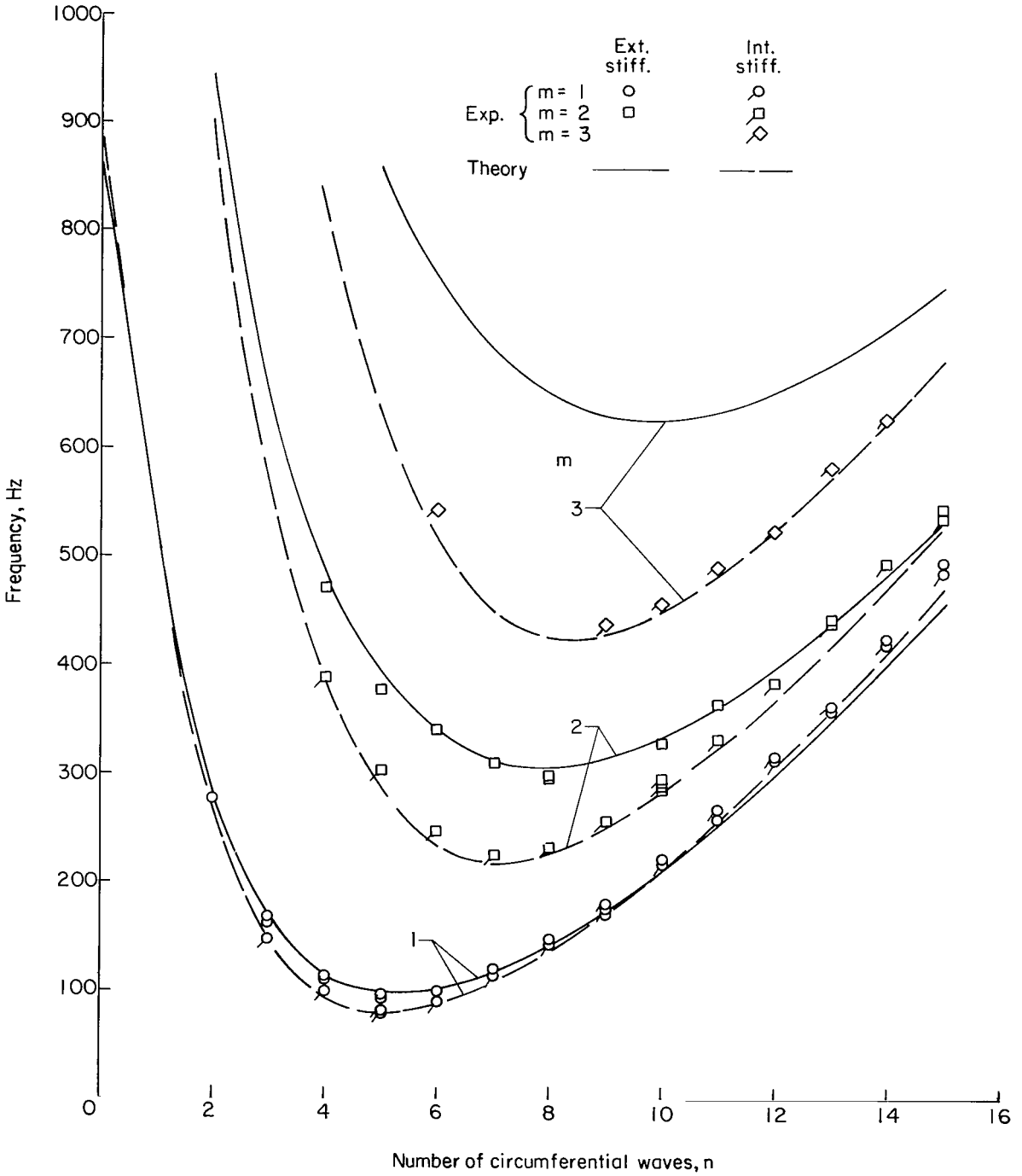

(b) Externally and internally stiffened shells.

Figure 11.- Concluded.

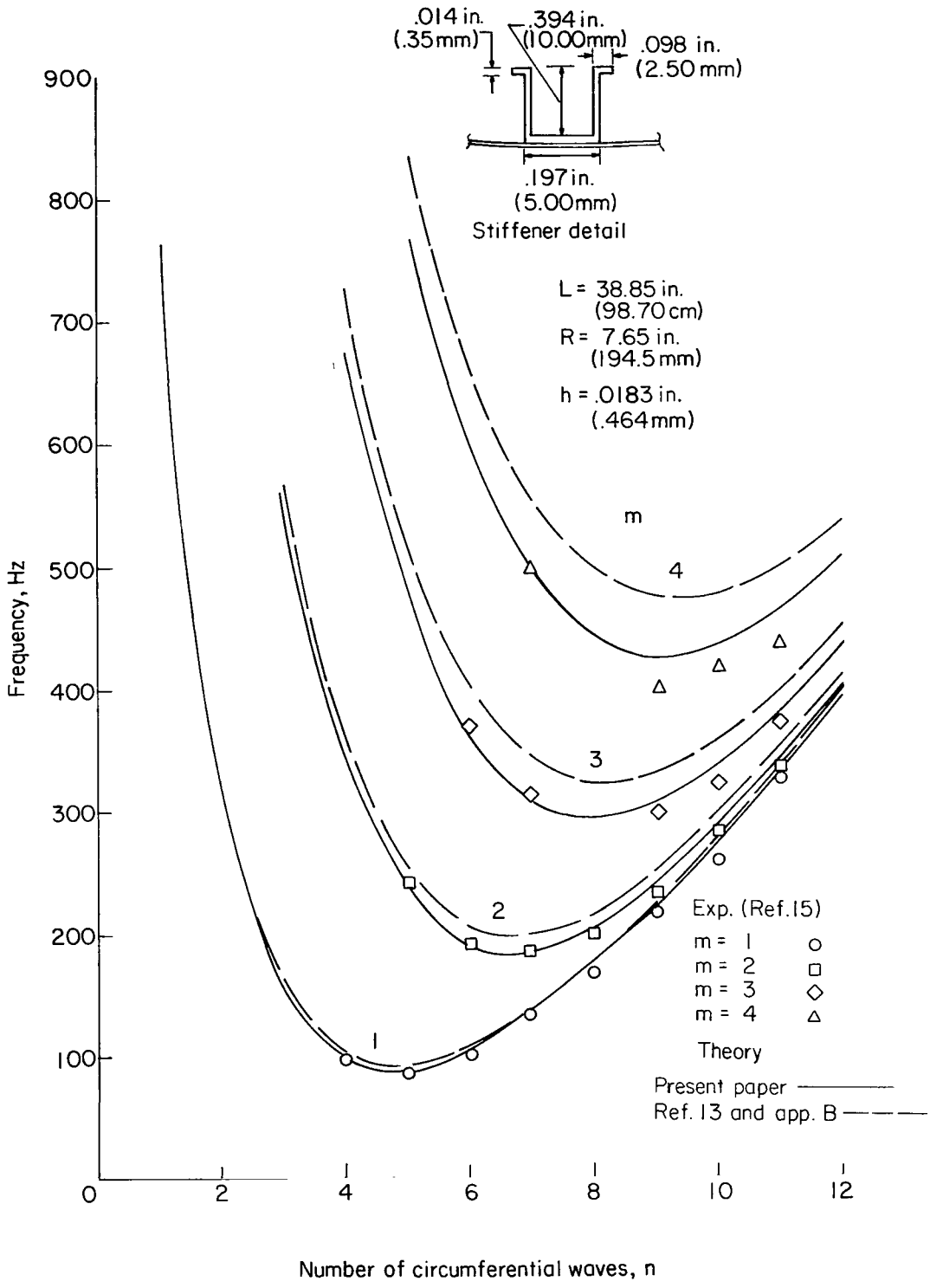

Figure 12.- Experimental and analytical frequencies of simply supported cylindrical shell with eight internal stringers.

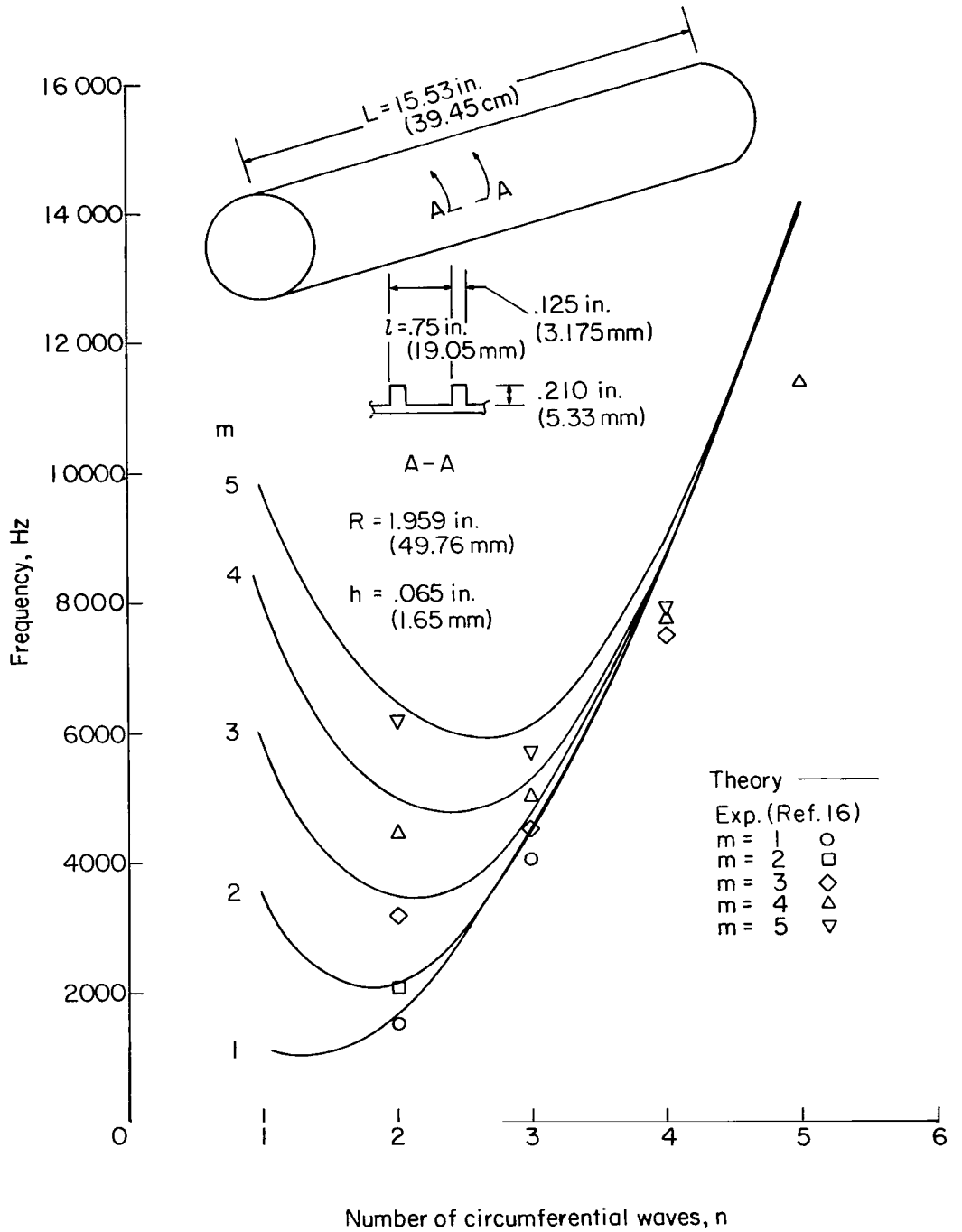

(a) Simply supported cylindrical shell stiffened by 19 integral rings.

Figure 13.- Experimental and analytical frequencies of ring-stiffened cylindrical shells.

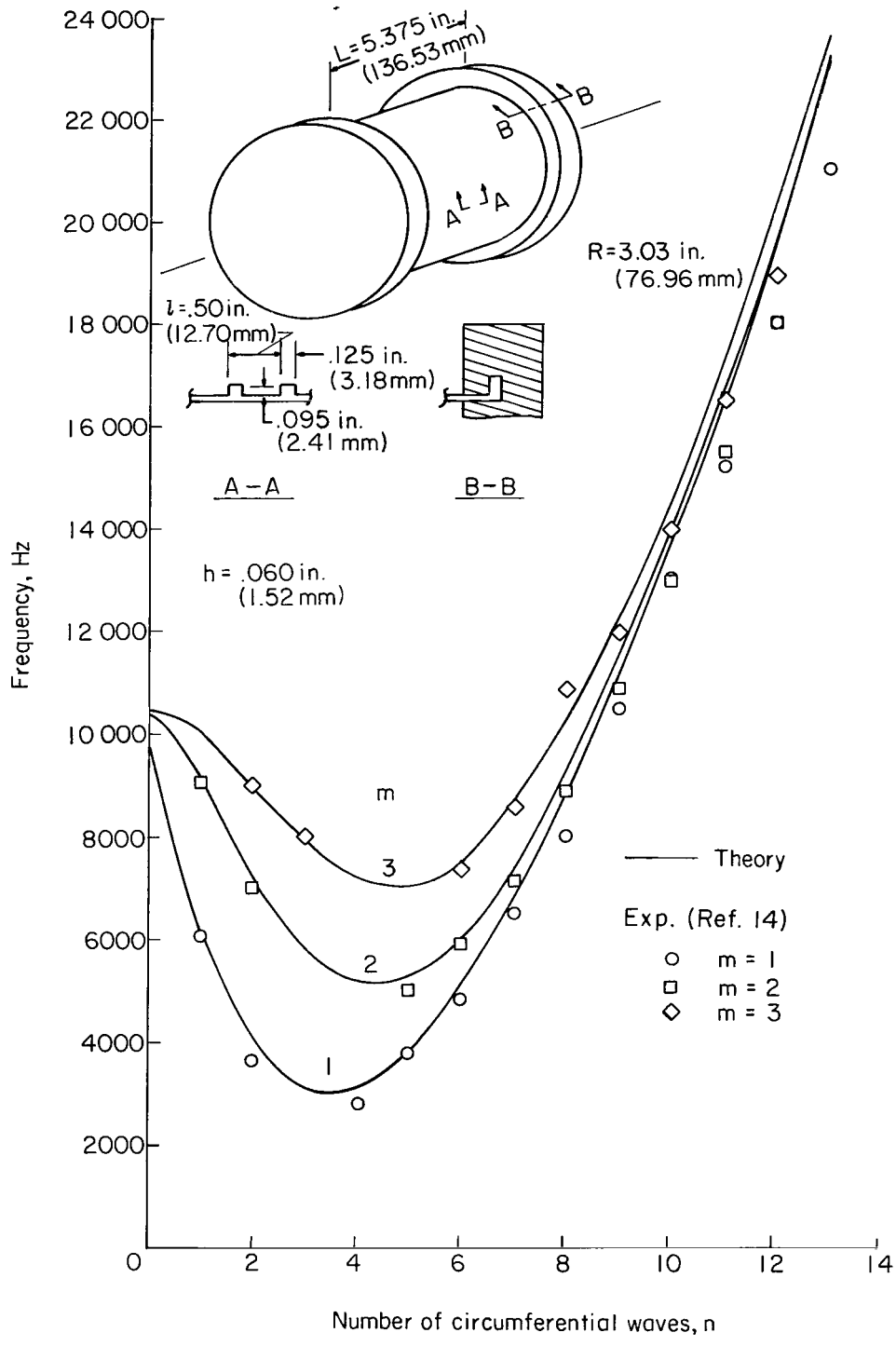

(b) Clamped-clamped cylindrical shell stiffened by 11 integral rings.

Figure 13.- Concluded.

NASA-Langley, 1968 —— 32 L-4583

NATIONAL AERONAUTICS AND SPACE ADMINISTRATION
WASHINGTON, D.C. 20546

OFFICIAL BUSINESS

FIRST CLASS MAIL

POSTAGE AND FEES PAID
NATIONAL AERONAUTICS AND
SPACE ADMINISTRATION

POSTMASTER: If Undeliverable (Section 158 Postal Manual) Do Not Return

"The aeronautical and space activities of the United States shall be conducted so as to contribute . . . to the expansion of human knowledge of phenomena in the atmosphere and space. The Administration shall provide for the widest practicable and appropriate dissemination of information concerning its activities and the results thereof."

—NATIONAL AERONAUTICS AND SPACE ACT OF 1958

NASA SCIENTIFIC AND TECHNICAL PUBLICATIONS

TECHNICAL REPORTS: Scientific and technical information considered important, complete, and a lasting contribution to existing knowledge.

TECHNICAL NOTES: Information less broad in scope but nevertheless of importance as a contribution to existing knowledge.

TECHNICAL MEMORANDUMS: Information receiving limited distribution because of preliminary data, security classification, or other reasons.

CONTRACTOR REPORTS: Scientific and technical information generated under a NASA contract or grant and considered an important contribution to existing knowledge.

TECHNICAL TRANSLATIONS: Information published in a foreign language considered to merit NASA distribution in English.

SPECIAL PUBLICATIONS: Information derived from or of value to NASA activities. Publications include conference proceedings, monographs, data compilations, handbooks, sourcebooks, and special bibliographies.

TECHNOLOGY UTILIZATION PUBLICATIONS: Information on technology used by NASA that may be of particular interest in commercial and other non-aerospace applications. Publications include Tech Briefs, Technology Utilization Reports and Notes, and Technology Surveys.

Details on the availability of these publications may be obtained from:

SCIENTIFIC AND TECHNICAL INFORMATION DIVISION

NATIONAL AERONAUTICS AND SPACE ADMINISTRATION

Washington, D.C. 20546